

1
2
3
4 **Increasing Temperature and Flow Management Alter Mercury Dynamics in**
5 **East Fork Poplar Creek**
6

7 Scott C. Brooks*¹, Carrie L. Miller², Ami L. Riscassi³, Kenneth A. Lowe¹,
8 Johnbull O. Dickson⁴, Grace E. Schwartz^{1†}
9

10
11 ¹Oak Ridge National Laboratory, Environmental Science Division. P.O. Box 2008, MS 6038, Oak Ridge,
12 TN, 37831-6038
13

14 ²Ramapo College of New Jersey, Theoretical and Applied Science, 505 Ramapo Valley Rd. Mahwah, NJ
15 07430
16

17 ³University of Virginia, Department of Environmental Sciences, 291 McCormick Rd, Charlottesville, VA,
18 22904
19

20 ⁴Florida International University, Applied Research Center, 10555 W. Flagler St, Miami, FL, 33174
21

22 †present address: Department of Chemistry, Wofford College, 429 N Church St, Spartanburg, SC 29303
23

24 *Corresponding Author: Email: brookssc@ornl.gov, Phone: 865-574-6398, Fax: 865-576-8646.
25

26 Research article submitted to: *Hydrological Processes*, Special Issue: “Research and Observatory
27 Catchments: The Legacy and the Future”
28

29
30 ***Disclaimer (not for publication)***

31 This manuscript has been authored by UT-Battelle, LLC under Contract No. DE-AC05-00OR22725 with
32 the US Department of Energy (DOE). The United States Government retains and the publisher, by
33 accepting the article for publication, acknowledges that the United States Government retains a non-
34 exclusive, paid-up, irrevocable, world-wide license to publish or reproduce the published form of this
35 manuscript, or allow others to do so, for United States Government purposes. The Department of Energy
36 will provide public access to these results of federally sponsored research in accordance with the DOE
37 Public Access Plan (<http://energy.gov/downloads/doe-public-access-plan>).
38
39

40
41
42
43
44
45
46
47
48
49
50
51
52
53
54
55
56
57
58
59
60
61
62
63
64
65
66

ABSTRACT

East Fork Poplar Creek (EFPC) is a mercury (Hg) contaminated creek in east Tennessee, USA. Stream restoration activities included the initiation of a flow management program in 1996 in which water from a nearby lake was pumped to the head of the creek. We conducted regular water sampling for two years along the length of EFPC during active flow management and for five years after flow management stopped. Total Hg and total monomethylmercury (MMHg) concentration and flux decreased in the uppermost reaches of EFPC that were closest to the point of water addition. Most water quality parameters, including DOC concentration, remained unchanged after flow management termination. Nevertheless, SUVA₂₅₄, a measure of dissolved organic matter (DOM) composition, increased and coincided with increased dissolved Hg (Hg_D) concentration and flux and decreased Hg solid-water partitioning coefficients throughout EFPC. Higher SUVA₂₅₄ and Hg_D concentration have potential implications for bioavailability and MMHg production. Total and dissolved MMHg concentrations increased in lower reaches of EFPC after the end of flow management and these increases were most pronounced during spring and early summer when biota are more susceptible to exposure and uptake. A general warming trend in the creek after active flow management ended likely acted in concert with higher Hg_D concentration to promote higher MMHg concentration. Total and dissolved MMHg concentrations were positively correlated with water temperature above a threshold value of 10 °C. Concentration changes for Hg and MMHg could not be accounted for by changes in creek discharge that accompanied the cessation of flow management. In addition to the changing DOM composition in-stream, other watershed-scale factors likely contributed to the observed patterns, as these changes occurred over months rather than instantaneously after flow management stopped. Nevertheless, similar changes in MMHg have not been observed in a tributary to EFPC.

67
68
69
70
71
72
73
74
75
76
77
78
79
80
81
82
83
84
85
86
87
88
89
90
91
92

INTRODUCTION

Mercury (Hg) has a complex biogeochemical cycle that has been substantially altered by anthropogenic activity (Obrist et al., 2018; Selin, 2009). Given that Hg mining dates back more than 3,000 years and its long-range atmospheric transport there may be few places on Earth’s surface that have not been impacted by alterations to its cycle (Beckers & Rinklebe, 2017) making Hg an element of concern at global, regional, and local scales. Additionally, globally there are more than 3,000 point-source contaminated systems owing to Hg-intensive uses such as mining, precious metal recovery, and manufacturing (Kocman, Horvat, Pirrone, & Cinnirella, 2013).

Inorganic Hg, the primary form released to the environment at most sites, has well-documented deleterious health effects. The transformation in the environment of inorganic mercury to the more toxic monomethylmercury (MMHg) increases the risks to human and environmental health. For these and other reasons, the United Nations Environment Programme lists contaminated site remediation as one of its seven priorities (United Nations Environment Programme Global Mercury Partnership, 2020). Understanding the controls on Hg transport and transformation informs fundamental understanding of biogeochemical cycles and is essential to addressing solutions for Hg contamination.

Both dissolved organic carbon (DOC) and total suspended solids (TSS) play important roles in Hg speciation and environmental chemistry (Dong, Bian, Liang, & Gu, 2011; Dong, Liang, Brooks, Southworth, & Gu, 2010; Gu et al., 2014; C. L. Miller, Liang, & Gu, 2012; C. L. Miller, Mason, Gilmour, & Heyes, 2007; Carrie L. Miller, Southworth, Brooks, Liang, & Gu, 2009). Dissolved organic matter (DOM) plays a central role in the behavior of Hg in the environment affecting sorption, precipitation and dissolution, and its propensity for methylation (Deonaraine & Hsu-Kim, 2009; Graham, Aiken, & Gilmour, 2013; Johs et al., 2019; Mitchell & Gilmour, 2008; Slowey, 2010; Waples, Nagy, Aiken, & Ryan, 2005). DOM composition, in addition to its concentration, is important with respect to Hg

93 biogeochemistry(Cumberland, Douglas, Grice, & Moreau, 2016; Sankar et al., 2019; Schuster et al.,
94 2008; Shiller, Duan, van Erp, & Bianchi, 2006). An indicator of DOM composition is the absorbance at
95 254 nm normalized to DOC concentration, referred to as SUVA₂₅₄. SUVA₂₅₄ has been positively
96 correlated to several DOM composition metrics including molecular weight, percent aromaticity, and
97 hydrophobicity (Wei et al., 2008; Weishaar et al., 2003). SUVA₂₅₄ also has been positively correlated
98 with total dissolved Hg concentration (Burns, Aiken, Bradley, Journey, & Schelker, 2013; Dittman et al.,
99 2009; Dittman et al., 2010; Eckley et al., 2018) and dissolution of the HgS mineral cinnabar has been
100 positively correlated with DOM molecular weight (Waples et al., 2005). Additionally, MMHg production
101 from inorganic Hg has been positively correlated with SUVA₂₈₀, a closely related metric (Mitchell &
102 Gilmour, 2008).

103

104 The strength and direction of the relationship between streamflow and Hg and MMHg concentrations has
105 been shown to vary depending on watershed characteristics and type and source of contamination.
106 Typically, higher flows suspend and transport more particulate matter resulting in increases in TSS and
107 the associated Hg and MMHg concentrations. This relationship has been documented in urban and non-
108 urban systems as well as in forested watersheds (Brigham, Wentz, Aiken, & Krabbenhoft, 2009), in
109 agricultural watersheds (Balogh, Huang, Offerman, Meyer, & Johnson, 2003), as well as in contaminated
110 systems with urban and forested components, such as EFPC (Ami Riscassi, Miller, & Brooks, 2016). An
111 exception to the increase in particulate Hg concentrations with increasing flow was observed in a logged
112 watershed (Eckley et al., 2018) with the unexpected absence of a trend attributed to best management
113 forestry practices designed to minimize erosion. The positive relationship between flow and dissolved Hg
114 is also fairly consistent, with higher flows activating previously dormant flowpaths and reconnecting
115 portions of the terrestrial watershed where the majority of Hg is stored (Brigham et al., 2009). The
116 relationship between flow and dissolved MMHg is more variable, with positive relationships found in
117 systems with a significant wetland abundance, in which methylmercury generation is greater in areas
118 outside of the stream channel that become connected, whereas negative relationships are more common in

119 systems without wetlands, in which in-stream methylation is dominant, including EFK-5 (see Figure 8a in
120 (Ami Riscassi et al., 2016)). Dominant watershed land-use also affects the strength of these relationships
121 with agricultural watersheds showing preferential increases in particulate concentrations and watersheds
122 with abundant wetlands having more prominent increases in dissolved concentrations (Babiarz et al.,
123 1998)

124

125 East Fork Poplar Creek (EFPC) in Oak Ridge, Tennessee, USA was heavily contaminated with mercury
126 (Hg) due to activities at the Y-12 National Security Complex (Y-12) located at the headwaters of the
127 creek (S. C. Brooks & Southworth, 2011; Loar, Stewart, & Smith, 2011). The creek and its watershed
128 have been the subject of intense monitoring, characterization, and research since the mid-1980's.

129 Numerous remedial actions have been taken and water quality within EFPC has improved but smaller
130 amounts of Hg continue to enter the creek from Y-12 and fish tissue concentrations throughout EFPC
131 remain above the US EPA guideline of $0.3 \mu\text{g g}^{-1}$. The water quality threat posed by Hg is related
132 primarily to its conversion to monomethylmercury (MMHg) and its subsequent bioaccumulation and
133 biomagnification posing a risk to top consumers.

134

135 Among the remedial actions taken in EFPC to address degraded stream ecology and water quality was the
136 initiation of a flow management program in August 1996 whose goal was to increase and stabilize the
137 minimum baseflow in the upper reaches of the creek. This goal was achieved by adding water from
138 Melton Hill Lake to the head of the creek at the rate of $0.2 \text{ m}^3 \text{ s}^{-1}$. The added lake water was 10-15 °C
139 cooler than EFPC at the point of mixing, was not a significant source of either total Hg or MMHg (long-
140 term mean 0.9 ng L^{-1} and 0.04 ng L^{-1} , respectively), and had higher TSS (long-term mean 5.8 mg L^{-1})
141 than EFPC (long-term mean 1 mg L^{-1}). Importantly, the added water had similar DOC concentration
142 (long-term means 1.54 mg L^{-1} , EFPC = 1.82 mg L^{-1}) but higher SUVA_{254} (long-term means 2.65 L mg-C^{-1}
143 m^{-1} , EFPC = $1.42 \text{ L mg-C}^{-1} \text{ m}^{-1}$) than EFPC at the point of addition. The flow management program
144 was stopped at the end of April 2014 to decrease total Hg flux leaving Y-12.

145
146
147
148
149
150
151
152
153
154
155
156
157
158
159
160
161
162
163
164
165
166
167
168
169
170

We conducted various sampling campaigns along EFPC during active flow management to characterize water quality, specifically Hg and MMHg behavior throughout the creek. Upon learning the flow additions would be terminated, the comprehensive sampling efforts were repeated for several years to document and quantify what, if any, changes to water quality occurred after flow management ended. Specifically, if changes to Hg and MMHg mobilization and/or formation occurred downstream of the headwaters after flow management modification, we sought to determine the factors contributing to those alterations. A combination of in-stream and broader climate-scale changes contributed to increased Hg and MMHg concentrations and fluxes after flow management ended.

METHODS

Site Description

The EFPC watershed is in the Valley and Ridge physiographic province of Tennessee and is underlain by limestone, dolostone, and shale bedrock. The region has a humid subtropical climate with mean annual temperature of 14.4 °C, mean annual precipitation of 137 cm that is evenly distributed throughout the year, and local evapotranspiration of 74-76 cm (Parr & Hughes, 2006). Streamflow exhibits strong seasonality due to high evapotranspiration from late March to mid-October (Mulholland et al., 1997). Land cover changes considerably from 87% developed, 11% forested in the upper reaches to 34% developed, 55% forested in the lower reaches. The high percentage of impervious cover in the upper part of the watershed results in flashy storm-driven hydrographs. EFPC is a fourth-order stream at the point of its confluence with Poplar Creek (Fig. 1). From its headwaters inside Y-12, the creek meanders 26 kilometers through commercial, residential, open-land and forested sections of the city of Oak Ridge, Tennessee to its confluence with Poplar Creek. The upper four creek kilometers have little canopy cover over the creek whereas much of the remaining 22 creek kilometers has heavy seasonal canopy cover from the deciduous trees populating the floodplain. Sampling sites are identified by an alphanumeric

171 designator EFK# where EFK stands for East Fork and the number signifies the creek kilometer, measured
172 upstream from the mouth of the creek. Halfway along its length (EFK 13.5), the city of Oak Ridge
173 Wastewater Treatment Facility (ORWTF) discharges treated water to the creek. Several perennial
174 tributaries are distributed along EFPC but discharge from the ORWTF constitutes the largest contributory
175 input to the EFPC main channel. This effluent is a source of nutrients (nitrate, ammonia, phosphorous)
176 and DOC to EFPC, but it is not a significant source of either Hg or MMHg. The reader is referred to
177 previous descriptions for more details (S. C. Brooks, Riscassi, & Lowe, 2021; S. C. Brooks &
178 Southworth, 2011; Loar et al., 2011; Ami Riscassi et al., 2016) .

179

180 **Field Methods**

181 Baseflow sampling along EFPC (Fig. 1) was conducted monthly at eleven sites from August 2010 to
182 December 2012 while flow management was on. The sampling was repeated from May 2014, after flow
183 augmentation was stopped, through August 2019. Sampling campaigns were conducted between 08:00
184 and 13:00 working from downstream to upstream. Ancillary tests did not show a significant difference
185 between downstream-to-upstream versus upstream-to-downstream sampling (Gammons, Milodragovich,
186 & Belanger-Woods, 2007). Bulk 500-mL water samples were collected in new PETG bottles by triple-
187 rinsing with creek water prior to sample collection. A separate sample for TSS was collected in a 2-liter
188 HDPE bottle. Samples were either processed immediately in the field or held on ice until returned to the
189 lab for processing [max holding time of 8 hours; (A. Riscassi, Miller, & Brooks, 2014)]. Concurrent with
190 water sampling, ambient water conditions were measured (temperature, specific conductance, pH,
191 dissolved oxygen; Table S1).

192

193 An unfiltered aliquot of each sample was retained for quantification of total Hg and MMHg (Hg_T and
194 $MMHg_T$, respectively) and the remaining sample was filtered through a 0.2 μm pore size polyethersulfone
195 filter for analysis of dissolved Hg and MMHg (Hg_D and $MMHg_D$, respectively), DOC, UV-Vis
196 absorption, anions, and metals. Samples collected for TSS analysis were filtered through a tared

197 Whatman GFF glass fiber filter with 0.7 μm particle retention. Unfiltered and filtered Hg and MMHg
198 samples were preserved to 0.5% (v/v) trace metal grade HCl in PETG bottles and DOC samples were
199 preserved to 0.1% (v/v) trace metal grade HCl in amber glass bottles. Samples for metals analysis were
200 acidified to 0.5% (v/v) with trace metal grade HNO_3 in either clear glass or LDPE bottles. Samples for
201 anion and UV-Vis analysis were kept in clear and amber glass bottles, respectively. All samples were
202 stored in the dark at 4 °C until analysis (Table S2). Field duplicates and equipment blanks were collected
203 for quality control during sampling events.

204

205 **Creek Discharge and Meteorological Data**

206 Mean daily stream discharge for EFK 24.3 was retrieved from the US Geological Survey (USGS ID#
207 03538235; period of record 1 December 1992 to 18 April 2005) and supplemented with data from the
208 Oak Ridge Environmental Information System (<https://oreis.ettp.energy.gov/>) and continuous discharge
209 records provided courtesy of Y-12 environmental compliance personnel. Mean daily discharge from the
210 ORWTF was provided courtesy of the City of Oak Ridge (1 November 1999 to 30 September 2019).
211 Continuous discharge and multiparameter sonde data at EFK 5.4 and 16.2 were collected at gauging
212 stations established by the authors (S. C. Brooks et al., 2021; Ami Riscassi et al., 2016)};
213 <https://www.esd.ornl.gov/programs/rsfa/data.shtml>). The downstream gauging station was a former
214 USGS water monitoring site (ID# 03538250) which operated from 1960 through June 1988 and for which
215 mean daily discharge records are available. Precipitation records for Oak Ridge, TN were obtained from
216 the Atmospheric Turbulence & Diffusion Division office of NOAA in Oak Ridge (ATDD, 1953 – 1988)
217 and National Weather Service (NWS) station KOQT (1989 – 2019). Hourly air temperature data for
218 station KOQT were retrieved from the North Carolina Climate Office, Weather and Climate Database
219 (<http://climate.ncsu.edu.cronos>).

220

221 **Analytical Methods**

222 Hg analyses were conducted following EPA method 1631 (U. S. EPA, 2002) using a Hg purge and trap
223 system (Brooks Rand MERX-T) (U. S. EPA, 2002). Ambient MMHg was analyzed using modifications
224 of EPA method 1630 (U. S. EPA, 2001). An internal standard (MM^{200}Hg) was added to samples prior to
225 distillation and this isotope was used to quantify MMHg concentrations (Hintelmann & Ogrinc, 2003). In
226 addition to analyzing the field duplicates and equipment blanks collected during sampling, analytical
227 replicates and spike recoveries were measured. A summary of Hg and MMHg quality assurance/quality
228 control results is given in supporting information (Table S3).

229

230 DOC concentrations were measured using high-temperature platinum-catalyzed combustion followed by
231 infrared detection of CO_2 (Shimadzu TOC-5000A or Shimadzu TOC-L). UV-visible spectra were
232 collected at 1-nm interval and 0.5 second exposure time from 190-1100 nm wavelength with an HP 8453
233 spectrophotometer using a 1-cm path length quartz cuvette. Dissolved anions (Cl^- , NO_3^- , SO_4^{2-} , PO_4^{3-})
234 and metals (Na, Mg, Ca, K, Al, Fe, Mn, Sr, Ba, U) were analyzed by ion chromatography (IC) (Dionex
235 DX-120, Sunnyville, CA, USA) and inductively coupled plasma-mass spectrometry (ICP-MS, Perkin-
236 Elmer, Waltham, MA, USA), respectively.

237

238 **Computations**

239 Statistics and calculations were conducted in R (R Core Team, 2018) using the RStudio IDE (RStudio
240 Team, 2018). Reported correlations are Spearman's rank correlation coefficient (ρ); where multiple
241 correlations were calculated, p values were adjusted using Holm's method. Particulate Hg and MMHg
242 were calculated both as (i) the difference between the total and dissolved concentration, reported in ng L^{-1}
243 ($\text{Hg}_{\text{p.ngL}}$ and $\text{MMHg}_{\text{p.ngL}}$, respectively), and (ii) the value from (i) divided by the TSS, reported as
244 milligrams Hg (or MMHg) per kilogram suspended solids (mg kg^{-1} ; $\text{Hg}_{\text{p.mgkg}}$ and $\text{MMHg}_{\text{p.mgkg}}$,
245 respectively). Solid-water partitioning coefficients (K_{SW} ; L kg^{-1}) were calculated as the ratio of solid
246 phase concentration to dissolved concentration:

247
$$K_{SW}(L\ kg^{-1}) = \frac{10^6 Hg_P(mg\ kg^{-1})}{Hg_D(mg\ L^{-1})} \quad Eq. 1$$

248 Results are reported as the $\log_{10}(K_{SW})$. This calculation is analogous to the K_D used to describe linear
249 sorption isotherms but differs in several important ways. A true K_D is an equilibrium measure of
250 adsorption made under constant conditions (e.g., pH, temperature). For the samples collected in this
251 study the equilibrium condition is uncertain, stream water chemistry varied over time and space, and
252 some of the particulate Hg may be in the form of (co-)precipitates in addition to being adsorbed on
253 particle surfaces.

254
255 Specific ultraviolet absorbance at 254 nm ($SUVA_{254}$), calculated as the absorbance at 254 nm (m^{-1})
256 divided by the DOC concentration ($mg\ L^{-1}$), is reported in units of $L\ mg^{-1}\ C^{-1}\ m^{-1}$. TSS ($mg\ L^{-1}$) was
257 determined by drying filters to constant weight at 60 °C and calculated by dividing the difference in mass
258 between the filter+TSS and the tare mass of the filter by the volume of water filtered. Instantaneous
259 material flux was calculated as the product of creek discharge at the time of sampling and the sample
260 concentration.

261
262 Seasons were assigned based on the solstices and equinoxes. Patterns and trends were evaluated for the
263 whole creek and for three individual reaches (upper, middle, lower; Fig. 1). The upper, middle, and lower
264 reaches encompassed 1.4, 4.4, and 4.5 kilometers and two, six, and three sampling sites, respectively.

265

266 **RESULTS**

267

268 **Creek discharge**

269 The flow management program was initiated to increase and stabilize the minimum baseflow at EFK
270 23.4. The success of that program in achieving its goal and the consequent effect of stopping the program
271 are evident in the discharge record (Fig. 2A; Table S4; Fig. S1A, S2A). The added water accounted for

272 ~80% of creek flow at the point where it entered EFPC and decreased to ~65% of creek flow at EFK 23.4
273 reflecting additional water inputs from the watershed plus minor additions from other permitted outfalls in
274 Y-12 over that 2.5 km distance. At EFK 23.4 the average mean daily discharge increased from 0.231 m^3
275 s^{-1} prior to the start of flow management (period of record 2.5 years) to $0.383 \text{ m}^3 \text{ s}^{-1}$ during the period of
276 active flow management (period of record 17 years) and decreased to $0.208 \text{ m}^3 \text{ s}^{-1}$ after flow management
277 termination (period of record 4.5 years). Flows were highest in the winter and lowest in summer and
278 autumn. The water added during flow management accounted for ~8.5% of mean daily discharge at EFK
279 5.4. That low percentage contribution coupled with gaps in the discharge record and the relatively short
280 record at EFK 5.4 during active flow management (period of record 2.3 years) make it hard to discern
281 what impact the termination of flow management may have had on discharge at that downstream location
282 (Fig. 2C; Fig. S1C, S2C). Average mean daily discharge at EFK 5.4 for the period of record during
283 active flow management ($1.91 \text{ m}^3 \text{ s}^{-1}$) was similar to discharge after flow management termination (1.87
284 $\text{m}^3 \text{ s}^{-1}$). Overall, discharge at EFK 5.4 was higher in the latter part of the total record (average mean daily
285 discharge from 2012-2019 = $1.88 \text{ m}^3 \text{ s}^{-1}$ versus $1.41 \text{ m}^3 \text{ s}^{-1}$ from 1960-1988). The higher flow from 2012
286 onward is likely due to a combination of higher precipitation in later years (mean annual rainfall for 2012-
287 2019 = 147 cm versus 135 cm for 1960-1988; Fig. S3) and higher runoff associated with changes in land
288 use and land cover with increasing watershed urbanization over time. Mean daily discharge from the
289 ORWTF was similar but slightly higher during the time flow management was on ($0.195 \text{ m}^3 \text{ s}^{-1}$) relative
290 to when it was off ($0.182 \text{ m}^3 \text{ s}^{-1}$; Fig. 2B).

291

292 ***Creek discharge during sampling***

293 Average mean daily discharge can be heavily influenced by a few moderate to high discharge events.
294 Notably, from 2016 to 2019, the Oak Ridge area experienced several 24-h periods with rainfall totals
295 exceeding 10 centimeters with correspondingly rare storm-driven floods whereas there was only one such
296 event when sampling occurred during active flow management. Instantaneous discharge at the time of
297 sampling (Q_{sample}) reveals different behavior and this information is necessary for the interpretation of the

298 water quality data. At EFK 23.4, Q_{sample} after flow management ended was about 50% of that during
299 active flow management (Fig. S4A, S30A). The greatest reduction in Q_{sample} occurred for summer
300 sampling (60% reduction) and the smallest reduction occurred in winter (43% reduction). At EFK 5.4, on
301 average there was no difference between Q_{sample} during versus after active flow management. However,
302 Q_{sample} in spring and summer was 10% and 22% lower, respectively, and winter Q_{sample} was 24% greater
303 after flow management ended (Fig. S4B, S30B). The lower range of Q_{sample} after flow management ended
304 was markedly lower than during active flow management: the lower 25th percentile of summer Q_{sample}
305 during active flow management ranged from 0.76 to 0.88 $\text{m}^3 \text{s}^{-1}$, and after flow management ended it
306 ranged from 0.53 to 0.67 $\text{m}^3 \text{s}^{-1}$, a 30 % decrease in the minimum value.

307

308 **EFPC Water Quality**

309 The addition of lake water to the head of EFPC successfully increased and stabilized baseflow at the point
310 where the creek exits Y-12. The higher flows also contributed to increased Hg flux primarily due to
311 increased mobilization of particulate Hg either by scouring and suspending contaminated sediments or
312 through Hg_D partitioning to the TSS added with the lake water. The flow management program was then
313 ended to achieve the desired goal of decreasing total mercury flux at baseflow from EFK 23.4 to the rest
314 of the watershed. From this perspective ending flow management, coupled with other remedial actions
315 within Y-12 to lower Hg concentration, has been successful (Fig. S5). Herein, we more closely examine
316 water quality changes throughout the rest of EFPC upon the cessation of the flow management program
317 and potential causes for those changes. These changes are examined for the whole creek and for three
318 reaches along the creek (Fig. 1).

319

320 ***Total, particulate, and dissolved Hg***

321 The general trends in Hg_T concentration along the length of EFPC were similar during and after flow
322 management. Hg_T concentration decreased downstream, and these longitudinal profiles were less steep
323 following the end of flow management due to lower concentrations at upstream locations (i.e., upstream

324 of the ORWTF outfall) and little to no change in Hg_T concentration in lower sections of the creek relative
325 to the active period of management (Fig. S7A, S7B, S8). This suggests that any concentration effect
326 associated with lower water volume in the upper section of the creek was offset by decreased particle-
327 associated Hg mobilization at lower flow resulting in a net decrease in Hg_T concentration. Both during
328 and after flow management Hg_T concentration was highest in the spring in the upper section of the creek
329 with smaller differences among seasons in the lower section of the creek. Seasonal patterns in Hg_T
330 concentration are evident with annual low values in late autumn to early winter increasing to springtime
331 maxima and decreasing through summer (Fig. S7, S8). In the upper reach, Hg_T was lower and less
332 variable after flow management ended and these changes were apparent immediately after flow
333 management ended. In the middle reach there was no apparent change in Hg_T concentration or variability
334 for the first 18 months after flow management ended. In the last few years of the record, the annual
335 maxima in the middle reach have decreased by half from 300 $ng\ L^{-1}$ to 150 $ng\ L^{-1}$. There has been no
336 apparent effect of flow management termination on Hg_T concentration in the lower reach. Hg_T and TSS
337 were positively correlated throughout EFPC (Table S6; whole creek: $\rho = 0.44$, $p < 0.001$; upper reach:
338 $\rho = 0.54$, $p < 0.001$; middle reach: $\rho = 0.67$, $p < 0.001$; lower reach: $\rho = 0.83$, $p < 0.001$)

339
340 The particle-specific Hg concentration ($Hg_{P.mgkg}$) showed a different response to flow management in each
341 of the three reaches (Fig. S9). In the upper reach, ongoing remedial activities in Y-12 decreased $Hg_{P.mgkg}$
342 while flow management was active. After flow management ended, the trend of decreasing $Hg_{P.mgkg}$
343 continued, reaching a relatively stable value of 26 $mg\ kg^{-1}$ about 18 months after the end of flow
344 management. In the middle reach $Hg_{P.mgkg}$ averaged 29 $mg\ kg^{-1}$ with no strong seasonal trend apparent
345 when flow management was active. Shortly after flow management ended $Hg_{P.mgkg}$ began to decrease
346 reaching a relatively stable value of 17 $mg\ kg^{-1}$ approximately 18 months after flow management ended.
347 In the lower reach, during active flow management mean $Hg_{P.mgkg}$ value was 16 $mg\ kg^{-1}$ and remained
348 variable but relatively steady for the initial 15 months after flow management ended. These values then
349 decreased over the next nine months after which they increased again to a mean value of 14 $mg\ kg^{-1}$.

350
351 Dissolved Hg concentration decreased with downstream distance for locations upstream of the ORWTF
352 outfall then remained relatively steady downstream of that point (Fig. S7C, S7D). Seasonal differences in
353 this trend were less apparent compared to Hg_T , although Hg_D concentration in autumn after flow
354 management stopped were lower than in the other seasons. Dissolved Hg concentration differed between
355 the upper and the middle and lower reaches and was relatively stable within each reach during active flow
356 management (Fig. 3). The upper, middle, and lower reaches had mean Hg_D of 36 ± 12 (excluding 2
357 winter outliers), 13 ± 3 , and 12 ± 4 $ng\ L^{-1}$, respectively. After flow management ended Hg_D
358 concentration remained stable for about six months then increased and became more variable in each
359 reach over the subsequent five years (Fig. 3; Fig. S7C, S7D). Samples in the latter part of the record
360 suggest that Hg_D concentration in the upper and middle reaches may have reached a new steady state of
361 ~ 100 and 30 $ng\ L^{-1}$, respectively. Nevertheless, intensive sampling in the lower reach in late summer
362 2018 showed ongoing high variability and increasing summertime maxima suggesting similar patterns
363 may also exist in the upper two reaches. The pattern of increasing Hg_D in each reach coupled with Hg_T
364 concentration changes yielded an increase in percent dissolved Hg (Hg_D/Hg_T) throughout EFPC after flow
365 management ended (Fig. S10). Additionally, the trends of decreasing $Hg_{P.mgkg}$ and increasing Hg_D lead to
366 decreasing $K_{SW.Hg}$ throughout EFPC (Eq. 1; Fig. 4) with the largest decrease occurring in the upper reach
367 followed by the middle and lower reaches. The trend of decreasing $K_{SW.Hg}$ occurred over the first three
368 years after flow management ended and then appears to have reached relatively stable values.

369

370 ***Total and dissolved MMHg***

371 $MMHg_T$ concentration increased with distance downstream both during and after active flow management
372 (Fig. S11A, S11B, S12). This longitudinal trend in $MMHg_T$ concentration is the opposite of that seen for
373 Hg_T . $MMHg_T$ was higher in spring and summer versus autumn and winter under both flow conditions
374 primarily due to a temperature-dependent biologically mediated MMHg production with potential
375 contribution from concentration effects related to lower creek discharge from late spring through early

376 autumn (Table S5; Fig. S2). MMHg_T concentration increased approximately linearly with downstream
377 distance in most cases except for spring and summer during flow management. In these latter two cases
378 MMHg_T increased rapidly in the first few creek kilometers then the rate of increase ($\text{ng L}^{-1} \text{ km}^{-1}$) declined
379 substantially over the remaining thirteen kilometers. Overall, the rate of MMHg_T increase with distance
380 downstream was higher after flow management ended due to lower concentrations in the upper reach and
381 higher concentrations in the middle and lower reaches.

382
383 Total MMHg concentration in the upper reach decreased and was less variable after flow management
384 stopped (Fig. S12). In contrast, MMHg_T in the middle and lower reaches were higher after flow
385 management ended. Strong seasonal effects are evident in the middle and lower reaches with annual
386 minima in late autumn and early winter. Concentrations increase through late winter to annual maxima in
387 late spring to early summer.

388
389 Dissolved MMHg concentration in the upper reach did not change after flow management ended. In the
390 middle and lower reaches MMHg_D increased after the end of flow management (Fig. 5). Higher
391 concentrations were measured in all seasons and annual minima and maxima progressively increased over
392 time. Increases in both $\text{MMHg}_{\text{P.mgkg}}$ and MMHg_D after flow management ended resulted in subtle but
393 significantly lower $K_{\text{SW.MMHg}}$ within each reach (Fig. S13; Tukey's Honestly Significant Difference test,
394 upper reach $\log K_{\text{SW.MMHg}}$ 0.2 lower, $p < 0.01$; middle reach $\log K_{\text{SW.MMHg}}$ 0.18 lower, $p < 0.01$; lower
395 reach $\log K_{\text{SW.MMHg}}$ 0.15 lower, $p < 0.01$).

396

397 *Additional water quality parameters*

398 When the flow management program was stopped, the addition of DOC and TSS to the head of the creek
399 was also eliminated. TSS concentration for samples collected in the upper reach during flow management
400 averaged $6.4 \pm 4.7 \text{ mg L}^{-1}$ (mean \pm standard deviation) (Fig. S14A). Post flow management, TSS
401 averaged $3.0 \pm 1.5 \text{ mg L}^{-1}$. The lower and less variable TSS after flow management ended was likely due

402 both to removal of the additional TSS loading and lower discharge that mobilized less suspended load
403 from the bed of EFPC. TSS values in the middle and lower reaches were not affected by flow
404 management (Fig. S14B, C). In all three reaches there were seasonal patterns in TSS concentration with
405 maxima in spring to early summer and minima in late autumn to early winter. TSS was not correlated
406 with discharge at EFK 23.4 ($\rho = 0.12$, $p = 0.44$) and weakly correlated with discharge at EFK 5.4 ($\rho =$
407 0.23 , $p < 0.05$) suggesting other factors controlled seasonal variation in TSS, although it should be noted
408 that the relatively narrow range of TSS and discharge values under the baseflow sampling regime may
409 bias the results of these correlations. The organic carbon content of TSS during flow management did not
410 exhibit any seasonal dependence suggesting that seasonal phytoplankton or zooplankton growth was not
411 the cause of seasonal variation in TSS.

412

413 DOC concentration showed no change throughout EFPC following flow management shutoff (Fig. S15).
414 DOC concentration in the flow management water was similar to that in EFPC just upstream of their
415 confluence. Consequently, terminating the flow management program decreased DOC loading to the
416 creek but did not alter DOC concentration in the upper reach ($1.7 \pm 0.9 \text{ mg-C L}^{-1}$). DOC concentration in
417 the middle reach ($1.7 \pm 1.2 \text{ mg-C L}^{-1}$) was similar to the upper reach. DOC concentration in the lower
418 reach ($2.3 \pm 0.9 \text{ mg-C L}^{-1}$; mean daily flux at EFK 5.4 $193 \pm 64 \text{ kg-C d}^{-1}$) was higher than in the upper or
419 middle reaches likely due to in-stream production and inputs from the forested watershed that dominates
420 the lower reach in addition to DOC loading from the ORWTF ($5.3 \pm 1.7 \text{ mg-C L}^{-1}$; mean daily flux
421 during sampling $69 \pm 16 \text{ kg-C d}^{-1}$).

422

423 Coincident with the end of flow management, SUVA_{254} values in all three reaches increased over an 18-
424 month period (Fig. 6) indicative of changing DOM composition. SUVA_{254} values for the lake water
425 added to the head of the creek during active flow management and for EFPC upstream of the point of
426 addition averaged $2.69 \text{ L mg-C}^{-1} \text{ m}^{-1}$ and $1.61 \text{ L mg-C}^{-1} \text{ m}^{-1}$, respectively. The patterns of increasing
427 SUVA_{254} mirror the pattern seen for changes in $K_{\text{SW,Hg}}$. pH and sulfate concentration were not affected by

428 the flow management termination. In the upper reach, chloride (excluding values associated with road
429 salt runoff) and nitrate concentrations increased 60% and 56%, respectively, reflecting a concentration
430 effect consistent with less dilution after active flow management ended (Fig. S16-S20). Specific
431 conductance in the upper reach increased 16% post-flow management. In the lower reach, chloride and
432 nitrate concentration concentrations increased 33% and 25%, respectively, and were more variable after
433 flow management. Lack of anion analyses for samples in the middle reach during active flow
434 management prevents similar comparisons.

435

436

DISCUSSION

437

Controls on Hg concentration: Creek discharge, particle suspension, solid-water partitioning

439 Stopping the addition of $0.2 \text{ m}^3 \text{ s}^{-1}$ water to the headwaters of EFPC had the desired effect of decreasing
440 total Hg concentration and flux at a point of regulatory compliance (EFK 23.4) and about 1.5 km
441 downstream of that point. Nevertheless, these benefits have not extended farther downstream as Hg_T
442 concentrations in the middle and lower reaches were not substantially different following the end of flow
443 management. Additionally, instantaneous flux of Hg_T , $\text{Hg}_{\text{P.ngL}}$, and Hg_D at the downstream gauging
444 station (EFK 5.4) was higher than at the upstream station (EFK 23.4) (Fig. S21, S30) both during and
445 after active flow management suggesting that diffuse legacy sources of Hg contamination along the
446 stream corridor sustain Hg concentration throughout much of EFPC at baseflow. Previous studies using
447 Hg stable isotope signatures (Demers et al., 2018) and mass balance approaches (S. C. Brooks et al.,
448 2018; Southworth et al., 2013) reported a similar conclusion. Recent studies of streambank soils and
449 streambed sediments along EFPC suggest that bank erosion of highly contaminated soils (up to 4600 mg-
450 Hg kg^{-1}) is a likely source of additional Hg inputs to the creek outside of Y-12 (S. Brooks et al., 2017;
451 Dickson et al., 2019). The patterns in Hg_T were similar to patterns in TSS leading to moderate to strong
452 positive correlations between these two variables for the whole creek and within each creek reach.
453 Numerous investigators have reported similar positive correlations between Hg concentration and TSS

454 (Brigham et al., 2009; Eckley et al., 2018; Hurley, Cowell, Shafer, & Hughes, 1998; Whyte & Kirchner,
455 2000).

456

457 Although changes to Hg_T concentration were limited to the upper reach, Hg_D concentration increased
458 throughout EFPC after the end of flow management. Increased Hg_D concentration in the upper reach
459 upon the end of flow management cannot be fully explained by a concentration effect due to cessation of
460 the diluting lake water additions. In that reach of EFPC, Hg_D concentrations did not start to increase until
461 nine months after, rather than immediately upon, the end of flow management. Hg_D instantaneous flux at
462 EFK 23.4 decreased in the first nine months after flow management ended (Fig. S21C) reflecting the
463 constant concentration and lower flow rate. After that period, Hg_D flux at EFK 23.4 increased as the
464 concentration increased and Q_{sample} remained relatively constant within each season. Cessation of flow
465 management had a much smaller impact on creek discharge at the downstream gauging station but Q_{sample}
466 was up to 22% lower after flow management ended (Fig. S4) which could have resulted in higher Hg_D
467 values by a concentration effect. Nevertheless, Hg_D instantaneous flux at EFK 5.4 increased after flow
468 management ended (Fig. S21C, S30F). Additionally, plotting Hg_D concentration versus Q_{sample} shows that
469 for a similar range of creek discharge, Hg_D concentration is substantially higher after cessation of flow
470 management (Fig. S22). Because of the temporal lag between the end of flow management and the onset
471 of increasing Hg_D concentrations throughout EFPC, higher Hg_D flux after flow management ended, and
472 the vertical offset in the concentration-discharge curve at EFK 5.4 factors other than a concentration
473 effect are responsible for the increasing Hg_D concentrations.

474

475 With the increasing Hg_D there was a corresponding decrease in partitioning onto the suspended solids as
476 estimated by $K_{SW,Hg}$. pH, ionic strength (IS), and DOC are recognized as master variables controlling
477 metal sorption behavior. However, pH, IS, and DOC were constant, showed little change, or do not show
478 directional changes with the termination of flow management that would explain the decreased Hg
479 partitioning (here, specific conductance is taken as a proxy measurement of ionic strength). Virtually all

480 the Hg_D in EFPC is expected to be associated with DOM (Dong et al., 2010) yet Hg_D was not correlated
481 with DOC in the upper or middle reaches, was moderately positively correlated in the lower reach and
482 was weakly negatively correlated with DOC considering the whole creek (Table S6). This result contrasts
483 with numerous other studies, conducted in non-point source contaminated watersheds, that reported
484 positive correlations between Hg_D and DOC in streams that span a broader range of DOC concentrations
485 and similar to narrower Hg_D concentration (Babiarz et al., 1998; Brigham et al., 2009; Dittman et al.,
486 2010; Journey et al., 2012; Oswald & Branfireun, 2014). Our results are in good agreement with those of
487 Lavoie et al. (Lavoie, Amyot, & Lapierre, 2019) who reported weaker Hg-DOC relationships in
488 anthropogenically impacted and point source contaminated systems suggesting that decoupling of Hg and
489 DOC sources and the ecosystem processes that include them changes the observed Hg-DOC relationship.
490 The change from no Hg-DOC correlation in the upper reaches to positive correlation in the lower reaches
491 corresponds to changes in watershed land cover from urban to forested.

492

493 $SUVA_{254}$ values for DOM from different sources may not mix conservatively, but it is noteworthy that
494 the added lake water had higher $SUVA_{254}$ values ($2.65 \text{ L mg-C}^{-1} \text{ m}^{-1}$) than EFPC upstream of the addition
495 point ($1.42 \text{ L mg-C}^{-1} \text{ m}^{-1}$) and that after flow management ended, $SUVA_{254}$ values increased in the upper,
496 middle, and lower reaches (Fig. 6). In our baseflow sampling of EFPC Hg_D was positively correlated
497 with $SUVA_{254}$ in all three creek reaches (Table S6). The correlation between these two variables for the
498 whole creek was much weaker. This suggests that even though DOC concentration remained relatively
499 steady, the change in DOM composition after flow management ended led to a corresponding lower
500 partitioning of Hg to suspended particles and higher Hg_D concentration. Similar to our results, Lavoie et
501 al. (Lavoie et al., 2019) reported stronger correlations between Hg and the aromatic fraction of DOM than
502 for Hg-DOC relationships. Changes to the TSS composition, particularly in the upper reach, also may
503 have contributed to the change in Hg partitioning behavior after flow management ended but there is no
504 TSS characterization data to make that comparison.

505

506 ***Controls on MMHg concentration: Creek discharge, available Hg, bacterial activity, and***
507 ***demethylation***

508 Lower MMHg_T concentration in the upper reach after the end of flow management was due to lower
509 MMHg_{p.ngL} concentration ($0.11 \pm 0.095 \text{ ng L}^{-1}$ and $0.034 \pm 0.036 \text{ ng L}^{-1}$ during and after active flow
510 management, respectively) as MMHg_D concentration did not change ($0.11 \pm 0.036 \text{ ng L}^{-1}$ and 0.1 ± 0.036
511 ng L^{-1} during and after active flow management, respectively). This suggests lower discharge scoured
512 and suspended less particle associated MMHg leading to lower MMHg_T concentration and lower MMHg_T
513 instantaneous flux at EFK 23.4 after flow management ended (Fig. S23A, S31A). Additionally, the loss
514 of the diluting lake water after flow management ended did not produce an associated concentration effect
515 for MMHg_D concentration and MMHg_{p.mgkg} was lower after flow management ended ($0.021 \pm 0.013 \text{ ng L}^{-1}$
516 1 and $0.013 \pm 0.0087 \text{ ng L}^{-1}$ during and after active flow management, respectively) suggesting less
517 MMHg_T in the upper reach after flow management ended. Instantaneous flux for MMHg_T, MMHg_{p.ngL},
518 and MMHg_D in at EFK 23.4 decreased after the end of flow management (Fig. S23, S31A&C).

519
520 In contrast to the decreasing MMHg_T and constant MMHg_D concentration in the upper reach, in the
521 middle and lower reaches MMHg_T and MMHg_D increased after flow management ended (Fig. 5, S12).
522 As was the case for inorganic Hg concentration, lower discharge at the time of sampling cannot explain
523 the concentration increase. At EFK 5.4 in the lower reach, for similar values of Q_{sample} , MMHg_D
524 concentration after flow management was substantially higher than during active flow management (Fig.
525 S24). Additionally, instantaneous flux of MMHg_T and MMHg_D at EFK 5.4 increased after flow
526 management ended (Fig. S23, S31B&D).

527
528 Because changes in creek discharge cannot account for changes in MMHg concentration, we address the
529 effects of other potential controls. MMHg is not a direct contaminant to EFPC but is formed in the
530 environment by a microbially-mediated process. Wetland abundance within a watershed is often found to
531 be an important source of MMHg to surface waters (Back, Hurley, & Rolffhus, 2002; Chasar, Scudder,

532 Stewart, Bell, & Aiken, 2009; Hurley et al., 1995; Krabbenhoft, Benoit, Babiarz, Hurley, & Andren,
533 1995; Scudder et al., 2009; Wentz, Brigham, Chasar, Lutz, & Krabbenhoft, 2014) with corresponding
534 positive correlations between basin wetland abundance and MMHg concentration. EFPC has
535 anomalously high MMHg concentration given the low wetland abundance (3%; National Wetland
536 Inventory) and previous research has concluded that MMHg in EFPC originates from in-stream sources
537 (Ami Riscassi et al., 2016).

538

539 Other watershed-scale variables affecting MMHg production include the concentration of available
540 inorganic Hg and the activity of methylating microorganisms. What constitutes Hg that is available for
541 methylation remains an unsettled question although there is general agreement that dissolved Hg is more
542 readily methylated than is Hg associated with particles (Hsu-Kim, Kucharzyk, Zhang, & Deshusses,
543 2013; Ndu et al., 2018; Zhang et al., 2011). Following flow management termination, Hg_D concentration
544 increased throughout EFPC which may have contributed to a pool of more readily methylated Hg
545 resulting in higher MMHg_D. However, MMHg concentration is uncorrelated and weakly negatively
546 correlated with Hg concentration for total and dissolved concentrations, respectively, when analyzing the
547 data without regard to location (Table S6; Fig. S25, S26). These correlation results for the whole creek
548 are expected given the longitudinal trends in the data (Fig. S5, S9). The dominant process affecting Hg
549 concentration along the length of the creek is dilution as new water enters EFPC along the stream
550 corridor. Legacy sources of Hg add to the total load of Hg at EFK 5.4 (Fig. S21) but have smaller impact
551 on concentration relative to the source from Y-12. Conversely, relatively little MMHg leaves Y-12 at
552 EFK 23.4 compared to the flux at EFK 5.4 (Fig. S23, S31). The dominant longitudinal process affecting
553 MMHg concentration is in-stream generation along the stream rather than dilution of a source term.

554

555 The counteracting processes of dilution of Hg versus generation of MMHg acting along the length of
556 EFPC mask relationships between Hg and MMHg when the whole creek is analyzed. Hence, the analysis
557 was repeated by creek reach and revealed relationships between Hg and MMHg that differed from the

558 whole creek analysis. In the upper reach MMHg_T and MMHg_D are positively correlated with Hg_T , no
559 correlation exists between MMHg_D and Hg_D , and there is a negative correlation between MMHg_T and
560 Hg_D . In the middle and lower reaches, MMHg and Hg are moderately positively correlated for all
561 combinations of total and dissolved concentrations (Table S6, Dig. S25, S26) although the MMHg_T - Hg_D
562 correlation in the middle reach is weak.

563
564 In addition to the relationships between SUVA_{254} , DOM composition, and inorganic Hg described earlier,
565 mercury methylation potential has been positively correlated with SUVA_{254} (Graham et al., 2013) and
566 SUVA_{280} (Mitchell & Gilmour, 2008), a closely related measure of DOM composition (Chin, Aiken, &
567 O'Loughlin, 1994). Additionally, the body burden of MMHg in benthic invertebrates and Hg_T in forage
568 fish and predator fish has been strongly positively correlated with SUVA_{254} (Chasar et al., 2009). The
569 precise mechanism by which DOM with higher SUVA values enhances methylation is unknown. It may
570 be related to the positive relationship between SUVA and Hg_D concentration and may include specific
571 effects on Hg-DOM uptake by methylating microorganisms (Mazrui, Jonsson, Thota, Zhao, & Mason,
572 2016) or non-specific stimulation of microbial metabolism. Despite the suggestion that higher SUVA_{254}
573 values could result in higher methylation potential, our data show moderate to weak negative correlations
574 (upper reach) to no correlation (middle and lower reaches) between SUVA_{254} and MMHg concentration
575 (Table S6). This may be due, in part, to the strong seasonal component to MMHg concentration that is
576 not apparent in the SUVA_{254} data.

577
578 Microbial activity and the processes the microbes mediate are positively correlated with temperature up to
579 group-specific thresholds (e.g., psychrophiles versus mesophiles versus thermophiles). This also holds
580 true for Hg methylation (Flanders et al., 2010; Olsen, Brandt, & Brooks, 2016; Schwartz, Olsen, Muller,
581 & Brooks, 2019; Tsui, Finlay, Balogh, & Nollet, 2010). For example, Flanders et al. reported Hg
582 methylation potentials in the South River, VA were low below a threshold temperature of 12°C and that
583 MMHg_D concentrations increased with temperature up to 24.7°C after which concentrations declined

584 (Flanders et al., 2010). In our EFPC dataset, MMHg concentration was low, relatively constant, and
585 independent of temperature for values below 10°C and was positively correlated with temperature above
586 that value (Table S7; Fig. 7, S27). In addition to noting this positive correlation, we evaluated trends in
587 air and stream temperature using the meteorological data and the continuous temperature data collected at
588 our instrumented gauging stations to calculate annual degree days using 10°C as the baseline reference
589 temperature. Degree days provide an estimate of heat accumulation over time. From 2013 to 2016
590 annual degree days in air and in EFPC increased 24% then remained elevated through 2019 (Fig. S28).
591 Mean temperature at EFK 5.4 increased from 15.4 °C in 2013 to 16.9 °C in 2019 and the number of days
592 per year when mean stream temperature exceeded 10 °C increased from 287 in 2013 to 328 in 2019. This
593 suggests that broader watershed warming created warmer stream temperatures and that over the seven-
594 year period, the time that stream temperature was in the range of positive correlation with MMHg
595 concentration steadily increased which could have contributed to increased MMHg production and
596 concentrations over the same period. The MMHg concentrations we measured are the net result of the
597 competing processes of Hg methylation and MMHg demethylation. Whereas Hg methylation is a
598 biologically mediated process, MMHg demethylation can proceed via either biotic or abiotic processes.
599 In EFPC periphyton biofilms, the biotic demethylation process is less temperature dependent than is
600 methylation, and net MMHg concentrations are driven largely by Hg methylation potential (Olsen et al.,
601 2016). Therefore, we expect the increase in degree days to favor net MMHg production.

602
603 The stream temperature data covaries with season and virtually all the samples with temperature below
604 10°C were collected in late autumn or in winter. Many other environmental variables that covary with
605 season such as periphyton growth, daily photoperiod length, light intensity, and canopy coverage can
606 affect in-stream processes, including net MMHg concentration. Previous work has shown that periphyton
607 biofilms can be an important source of MMHg in freshwater aquatic ecosystems, including in EFPC
608 (Achá, Hintelmann, & Yee, 2011; Desrosiers, Planas, & Mucci, 2006; S. Hamelin, Planas, & Amyot,
609 2015; S. p. Hamelin, Amyot, Barkay, Wang, & Planas, 2011; Huguet et al., 2010; Lazaro, Diez, da Silva,

610 Ignacio, & Guimaraes, 2018; Olsen et al., 2016; Schwartz et al., 2019). Higher springtime MMHg
611 concentration may be due, in part, to more abundant periphyton coverage on the streambed in that season
612 and associated MMHg production in those biofilms. The time of more abundant periphyton growth and
613 higher MMHg concentration coincides with low canopy coverage over the channel, increasing stream
614 temperature, increasing light intensity, and lengthening days. Numerous scientists have demonstrated that
615 photodemethylation, the abiotic process by which UV light cleaves the Hg-C bond in MMHg, resulted in
616 lower daytime MMHg concentrations compared to overnight concentrations (Fleck et al., 2009; Naftz et
617 al., 2011; Qian et al., 2014; Sellers, Kelly, Rudd, & MacHutchon, 1996). Nevertheless, previous research
618 has demonstrated the opposite trend in EFPC with daytime MMHg concentration maxima and overnight
619 minima at EFK 23.4 and EFK 5.4 (S. C. Brooks et al., 2018). These intraday patterns in MMHg
620 concentration in EFPC are evident in summer, weaken through autumn, and are absent in winter. The
621 daily range in MMHg concentration increases with downstream distance which may be related to higher
622 canopy coverage in downstream sections of the creek that limits the effects of photodemethylation during
623 the day. Nimick et al. also reported daytime maxima and overnight minima in MMHg concentration for
624 two streams in Montana that had relatively little canopy cover (Nimick, McCleskey, Gammons, Cleasby,
625 & Parker, 2007). Therefore, the conditions that develop in springtime, in addition to increasing
626 temperature, promote higher MMHg concentration.

627
628 Our results point to a combination of in-stream (increasing SUVA₂₅₄) and broader climate changes
629 (increasing degree days) after flow management ended that have resulted in higher MMHg
630 concentrations. These effects appear to be limited to the main channel of EFPC as similar changes across
631 parameters were not observed in Mill Branch, a perennial tributary in the middle reach (Fig. 1).

632 Following the end of flow management, Hg_D concentration nearly doubled in Mill Branch (0.45 ± 0.19 ng
633 L⁻¹, 0.86 ± 0.29 ng L⁻¹, flow management on and off, respectively) but there were no changes to either
634 SUVA₂₅₄ or MMHg_D similar to what was observed in EFPC (Fig. S29). The difference in MMHg
635 patterns between Mill Branch and the main channel of EFPC may also depend on differences in the

636 source of Hg (primarily atmospheric deposition in Mill Branch (Donovan et al., 2014)) and differences in
637 hydrology of the subwatershed compared to that of the entire watershed.

638
639 Following the end of flow management Hg_T concentration at locations closest to the headwaters
640 decreased and Hg_D concentration increased throughout EFPC. Additionally, MMHg concentrations
641 increased in the middle and lower reaches. These changes coincided with increases in $SUVA_{254}$ and a
642 general warming trend in the watershed. Increasing $SUVA_{254}$ values in EFPC, indicative of changes to
643 DOM composition, were positively correlated with Hg_D concentration which, in turn, increased the size of
644 the pool of more readily methylated Hg. Higher $SUVA_{254}$ values also have been correlated with higher
645 methylation rates. We suggest that the increase in $SUVA_{254}$ contributed to changes in Hg speciation
646 (increased Hg_D) and to MMHg production. The combined effect of the in-stream and watershed-scale
647 changes that occurred after flow management stopped drove higher MMHg concentration throughout
648 much of EFPC. Additionally, the vertical offset in the concentration-discharge curves and flux
649 exceedance probability curves for Hg_D and $MMHg_D$ implies increased loading of these constituents to
650 EFPC after active flow management stopped (Kirchner, Austin, Myers, & Whyte, 2011; Whyte &
651 Kirchner, 2000). Finally, the temperature-dependent changes to Hg behavior and MMHg generation have
652 broader implications for studies of aquatic systems, site characterization, remediation, and monitoring.
653 Rising temperatures can reverse the course of ecosystem recovery following targeted actions at
654 contaminated sites or decreased atmospheric deposition. Directional changes in controlling variables and
655 the timing and distribution of stochastic weather events should be considered in the interpretation of
656 similar long-term data records.

657

658

DATA AVAILABILITY STATEMENT

659

660 The water quality data and accompanying metadata are publicly available at
661 <https://msfa.ornl.gov/data/pages/MCI538.html>. The monitoring program is ongoing and evolving. For
662 additional information please contact the corresponding author at brookssc@ornl.gov.

663

664

ACKNOWLEDGMENTS

665

666 This work was funded by the U.S. Department of Energy, Office of Science, Biological and
667 Environmental Research, Subsurface Biogeochemical Research (SBR) Program, the U.S. Department of
668 Energy's Oak Ridge Office of Environmental Management (OROEM), and URS | CH2M Oak Ridge
669 LLC (UCOR). The isotopes used in this research were supplied by the United States Department of
670 Energy Office of Science by the Isotope Program in the Office of Nuclear Physics. Oak Ridge National
671 Laboratory is managed by UT-Battelle, LLC, for the U.S. Department of Energy under contract DE-
672 AC05-00OR22725.

673
674
675
676
677
678
679
680
681
682
683
684
685
686
687
688
689
690
691
692
693
694
695
696
697
698
699
700
701
702
703
704
705
706
707
708
709
710
711
712
713
714
715
716
717
718
719
720
721

REFERENCES

- Achá, D., Hintelmann, H., & Yee, J. (2011). Importance of sulfate reducing bacteria in mercury methylation and demethylation in periphyton from Bolivian Amazon region. *Chemosphere*, 82(6), 911-916.
- Babiarz, C. L., Hurley, J. P., Benoit, J. M., Shafer, M. M., Andren, A. W., & Webb, D. A. (1998). Seasonal influences on partitioning and transport of total and methylmercury in rivers from contrasting watersheds. *Biogeochemistry*, 41(3), 237-257.
- Back, R. C., Hurley, J. P., & Rolffhus, K. R. (2002). Watershed influences on the transport, fate and bioavailability of mercury in Lake Superior: Field measurements and modelling approaches. *Lakes & Reservoirs: Science, Policy and Management for Sustainable Use*, 7(3), 201-206. doi:10.1046/j.1440-1770.2002.00188.x
- Balogh, S. J., Huang, Y., Offerman, H. J., Meyer, M. L., & Johnson, D. K. (2003). Methylmercury in rivers draining cultivated watersheds. *Science of The Total Environment*, 304(1), 305-313. doi:[https://doi.org/10.1016/S0048-9697\(02\)00577-6](https://doi.org/10.1016/S0048-9697(02)00577-6)
- Beckers, F., & Rinklebe, J. (2017). Cycling of mercury in the environment: Sources, fate, and human health implications: A review. *Critical Reviews in Environmental Science and Technology*, 47(9), 693-794. doi:10.1080/10643389.2017.1326277
- Brigham, M. E., Wentz, D. A., Aiken, G. R., & Krabbenhoft, D. P. (2009). Mercury Cycling in Stream Ecosystems. 1. Water Column Chemistry and Transport. *Environ. Sci. Technol.*, 43(8), 2720-2725. doi:10.1021/es802694n
- Brooks, S., Eller, V., Dickson, J. O., Earles, J., Lowe, K., Mehlhorn, T., . . . Peterson, M. (2017). *Mercury Content of Sediments in East Fork Poplar Creek: Current Assessment and Past Trends. ORNL/TM-2016/578*. Retrieved from Oak Ridge National Laboratory. doi: 10.2172/1338545:
- Brooks, S. C., Lowe, K. A., Mehlhorn, T. L., Olsen, T. A., Yin, X., Fortner, A. M., & Peterson, M. J. (2018). *Intraday water quality patterns in East Fork Poplar Creek with an emphasis on mercury and monomethylmercury. ORNL/TM-2018/812*. Retrieved from Oak Ridge National Laboratory. doi: 10.2172/1437608:
- Brooks, S. C., Riscassi, A. L., & Lowe, K. A. (2021). Stream discharge and water quality data for East Fork Poplar Creek beginning 2012. *Hydrological Processes*, 35(3), e14103. doi:<https://doi.org/10.1002/hyp.14103>
- Brooks, S. C., & Southworth, G. R. (2011). History of mercury use and environmental contamination at the Oak Ridge Y-12 Plant. *Environ. Poll.*, 159(1), 219-228. doi:10.1016/j.envpol.2010.09.009
- Burns, D. A., Aiken, G. R., Bradley, P. M., Journey, C. A., & Schelker, J. (2013). Specific ultra-violet absorbance as an indicator of mercury sources in an Adirondack River basin. *Biogeochemistry*, 113(1), 451-466. doi:10.1007/s10533-012-9773-5
- Chasar, L. C., Scudder, B. C., Stewart, A. R., Bell, A. H., & Aiken, G. R. (2009). Mercury Cycling in Stream Ecosystems. 3. Trophic Dynamics and Methylmercury Bioaccumulation. *Environ. Sci. Technol.*, 43(8), 2733-2739. doi:10.1021/es8027567
- Chin, Y.-P., Aiken, G., & O'Loughlin, E. (1994). Molecular Weight, Polydispersity, and Spectroscopic Properties of Aquatic Humic Substances. *Environmental Science & Technology*, 28(11), 1853-1858. doi:10.1021/es00060a015
- Cumberland, S. A., Douglas, G., Grice, K., & Moreau, J. W. (2016). Uranium mobility in organic matter-rich sediments: A review of geological and geochemical processes. *Earth-Science Reviews*, 159, 160-185. doi:<https://doi.org/10.1016/j.earscirev.2016.05.010>
- Demers, J. D., Blum, J. D., Brooks, S. C., Donovan, Patrick M., Riscassi, A. L., Miller, C. L., . . . Gu, B. (2018). Hg isotopes reveal in-stream processing and legacy inputs in East Fork Poplar Creek, Oak Ridge, Tennessee, USA. *Environmental Science: Processes & Impacts*, 20(4), 686-707. doi:10.1039/C7EM00538E

- 722 Deonaraine, A., & Hsu-Kim, H. (2009). Precipitation of Mercuric Sulfide Nanoparticles in NOM-
 723 Containing Water: Implications for the Natural Environment. *Environ. Sci. Technol.*, *43*(7), 2368-
 724 2373. doi:10.1021/es803130h
- 725 Desrosiers, M., Planas, D., & Mucci, A. (2006). Mercury Methylation in the Epilithon of Boreal Shield
 726 Aquatic Ecosystems. *Environmental Science & Technology*, *40*(5), 1540-1546.
 727 doi:10.1021/es0508828
- 728 Dickson, J. O., Mayes, M. A., Brooks, S. C., Mehlhorn, T. L., Lowe, K. A., Earles, J. K., . . . Peterson, M.
 729 J. (2019). Source relationships between streambank soils and streambed sediments in a mercury-
 730 contaminated stream. *J. Soils Sediments*, *19*(4), 2007-2019. doi:10.1007/s11368-018-2183-0
- 731 Dittman, J. A., Shanley, J. B., Driscoll, C. T., Aiken, G. R., Chalmers, A. T., & Towse, J. E. (2009).
 732 Ultraviolet absorbance as a proxy for total dissolved mercury in streams. *Environ. Pollut.*, *157*(6),
 733 1953-1956.
- 734 Dittman, J. A., Shanley, J. B., Driscoll, C. T., Aiken, G. R., Chalmers, A. T., Towse, J. E., & Selvendiran,
 735 P. (2010). Mercury dynamics in relation to dissolved organic carbon concentration and quality
 736 during high flow events in three northeastern U.S. streams. *Water Resources Research*, *46*(7).
 737 doi:10.1029/2009wr008351
- 738 Dong, W. M., Bian, Y. R., Liang, L. Y., & Gu, B. H. (2011). Binding Constants of Mercury and
 739 Dissolved Organic Matter Determined by a Modified Ion Exchange Technique. *Environ. Sci.*
 740 *Technol.*, *45*(8), 3576-3583. doi:10.1021/es104207g
- 741 Dong, W. M., Liang, L. Y., Brooks, S., Southworth, G., & Gu, B. H. (2010). Roles of dissolved organic
 742 matter in the speciation of mercury and methylmercury in a contaminated ecosystem in Oak
 743 Ridge, Tennessee. *Environmental Chemistry*, *7*(1), 94-102.
- 744 Donovan, P. M., Blum, J. D., Demers, J. D., Gu, B. H., Brooks, S. C., & Peryam, J. (2014). Identification
 745 of Multiple Mercury Sources to Stream Sediments near Oak Ridge, TN, USA. *Environ. Sci.*
 746 *Technol.*, *48*(7), 3666-3674. doi:10.1021/es4046549
- 747 Eckley, C. S., Eagles-Smith, C., Tate, M. T., Kowalski, B., Danehy, R., Johnson, S. L., & Krabbenhoft,
 748 D. P. (2018). Stream Mercury Export in Response to Contemporary Timber Harvesting Methods
 749 (Pacific Coastal Mountains, Oregon, USA). *Environmental Science & Technology*.
 750 doi:10.1021/acs.est.7b05197
- 751 Flanders, J. R., Turner, R. R., Morrison, T., Jensen, R., Pizzuto, J., Skalak, K., & Stahl, R. (2010).
 752 Distribution, behavior, and transport of inorganic and methylmercury in a high gradient stream.
 753 *Appl. Geochem.*, *25*(11), 1756-1769.
- 754 Fleck, J. A., Downing, B. D., Saraceno, J. F., Gill, G., Stephenson, M., Alpers, C. N., & Bergamaschi, B.
 755 A. (2009). *Diurnal trends in methylmercury concentration and organic matter photo-reactivity in*
 756 *agricultural wetlands of the Yolo Bypass, California*. Paper presented at the Geological Society of
 757 America Annual Meeting, 18-21 October 2009, Portland, OR.
- 758 Gammons, C. H., Milodragovich, L., & Belanger-Woods, J. (2007). Influence of diurnal cycles on metal
 759 concentrations and loads in streams draining abandoned mine lands: an example from High Ore
 760 Creek, Montana. *Environmental Geology*, *53*(3), 611-622. doi:10.1007/s00254-007-0676-z
- 761 Graham, A. M., Aiken, G. R., & Gilmour, C. C. (2013). Effect of Dissolved Organic Matter Source and
 762 Character on Microbial Hg Methylation in Hg-S-DOM Solutions. *Environmental Science &*
 763 *Technology*, *47*(11), 5746-5754. doi:10.1021/es400414a
- 764 Gu, B., Mishra, B., Miller, C., Wang, W., Lai, B., Brooks, S. C., . . . Liang, L. (2014). X-ray fluorescence
 765 mapping of mercury on suspended mineral particles and diatoms in a contaminated freshwater
 766 system. *Biogeosciences*, *11*(18), 5259-5267. doi:10.5194/bg-11-5259-2014
- 767 Hamelin, S., Planas, D., & Amyot, M. (2015). Mercury methylation and demethylation by periphyton
 768 biofilms and their host in a fluvial wetland of the St. Lawrence River (QC, Canada). *Science of*
 769 *The Total Environment*, *512-513*(0), 464-471.
 770 doi:<http://dx.doi.org/10.1016/j.scitotenv.2015.01.040>

- 771 Hamelin, S. p., Amyot, M., Barkay, T., Wang, Y., & Planas, D. (2011). Methanogens: Principal
 772 Methylators of Mercury in Lake Periphyton. *Environ. Sci. Technol.*, 45(18), 7693-7700.
 773 doi:10.1021/es2010072
- 774 Hintelmann, H., & Ogrinc, N. (2003). Determination of stable mercury isotopes by ICP/MS and their
 775 application in environmental studies. In Y. Cai & O. C. Braids (Eds.), *Biogeochemistry of*
 776 *Environmentally Important Trace Elements* (Vol. 835, pp. 321-338). Washington: Amer
 777 Chemical Soc.
- 778 Hsu-Kim, H., Kucharzyk, K. H., Zhang, T., & Deshusses, M. A. (2013). Mechanisms Regulating
 779 Mercury Bioavailability for Methylating Microorganisms in the Aquatic Environment: A Critical
 780 Review. *Environmental Science & Technology*, 47(6), 2441-2456. doi:10.1021/es304370g
- 781 Huguet, L., Castelle, S., Schafer, J., Blanc, G., Maury-Brachet, R., Reynouard, C., & Jorand, F. (2010).
 782 Mercury methylation rates of biofilm and plankton microorganisms from a hydroelectric reservoir
 783 in French Guiana. *Science of The Total Environment*, 408(6), 1338-1348.
 784 doi:10.1016/j.scitotenv.2009.10.058
- 785 Hurley, J. P., Benoit, J. M., Babiarz, C. L., Shafer, M. M., Andren, A. W., Sullivan, J. R., . . . Webb, D.
 786 A. (1995). Influences of watershed characteristics on mercury levels in Wisconsin Rivers.
 787 *Environ. Sci. Technol.*, 29(7), 1867-1875.
- 788 Hurley, J. P., Cowell, S. E., Shafer, M. M., & Hughes, P. E. (1998). Partitioning and transport of total and
 789 methyl mercury in the Lower Fox River, Wisconsin. *Environ. Sci. Technol.*, 32(10), 1424-1432.
- 790 Johs, A., Eller, V. A., Mehlhorn, T. L., Brooks, S. C., Harper, D. P., Mayes, M. A., . . . Peterson, M. J.
 791 (2019). Dissolved organic matter reduces the effectiveness of sorbents for mercury removal.
 792 *Science of The Total Environment*, 690, 410-416.
 793 doi:<https://doi.org/10.1016/j.scitotenv.2019.07.001>
- 794 Journey, C. A., Burns, D. A., Riva-Murray, K., Brigham, M. E., Button, D. T., Feaster, T. D., . . . Bradley,
 795 P. M. (2012). *Fluvial transport of mercury, organic carbon, suspended sediment, and selected*
 796 *major ions in contrasting stream basins in South Carolina and New York, October 2004 to*
 797 *September 2009* (U.S. Geological Survey Scientific Investigations Report 2012–5173). Retrieved
 798 from
- 799 Kirchner, J. W., Austin, C. M., Myers, A., & Whyte, D. C. (2011). Quantifying Remediation
 800 Effectiveness under Variable External Forcing Using Contaminant Rating Curves. *Environ. Sci.*
 801 *Technol.*, 45(18), 7874-7881. doi:10.1021/es2014874
- 802 Kocman, D., Horvat, M., Pirrone, N., & Cinnirella, S. (2013). Contribution of contaminated sites to the
 803 global mercury budget. *Environmental Research*, 125, 160-170.
 804 doi:<https://doi.org/10.1016/j.envres.2012.12.011>
- 805 Krabbenhoft, D. P., Benoit, J. M., Babiarz, C. L., Hurley, J. P., & Andren, A. W. (1995). Mercury cycling
 806 in the Allequash Creek watershed, northern Wisconsin. *Water, Air, and Soil Pollution*, 80(1),
 807 425-433. doi:10.1007/BF01189692
- 808 Lavoie, R. A., Amyot, M., & Lapierre, J.-F. (2019). Global Meta-Analysis on the Relationship Between
 809 Mercury and Dissolved Organic Carbon in Freshwater Environments. *Journal of Geophysical*
 810 *Research: Biogeosciences*, 124(6), 1508-1523. doi:<https://doi.org/10.1029/2018JG004896>
- 811 Lazaro, W. L., Diez, S., da Silva, C. J., Ignacio, A. R. A., & Guimaraes, J. R. D. (2018). Seasonal changes
 812 in peryphytic microbial metabolism determining mercury methylation in a tropical wetland.
 813 *Science of The Total Environment*, 627, 1345-1352. doi:10.1016/j.scitotenv.2018.01.186
- 814 Loar, J. M., Stewart, A. J., & Smith, J. G. (2011). Twenty-Five Years of Ecological Recovery of East
 815 Fork Poplar Creek: Review of Environmental Problems and Remedial Actions. *Environ.*
 816 *Management*, 47(6), 1010-1020. doi:10.1007/s00267-011-9625-4
- 817 Mazrui, N. M., Jonsson, S., Thota, S., Zhao, J., & Mason, R. P. (2016). Enhanced availability of mercury
 818 bound to dissolved organic matter for methylation in marine sediments. *Geochimica et*
 819 *Cosmochimica Acta*, 194, 153-162. doi:<https://doi.org/10.1016/j.gca.2016.08.019>

- 820 Miller, C. L., Liang, L. Y., & Gu, B. H. (2012). Competitive ligand exchange reveals time dependant
 821 changes in the reactivity of Hg-dissolved organic matter complexes. *Environmental Chemistry*,
 822 9(6), 495-501. doi:10.1071/en12096
- 823 Miller, C. L., Mason, R. P., Gilmour, C. C., & Heyes, A. (2007). Influence of dissolved organic matter on
 824 the complexation of mercury under sulfidic conditions. *Environ. Toxicol. Chem.*, 26(4), 624-633.
- 825 Miller, C. L., Southworth, G. R., Brooks, S. C., Liang, L., & Gu, B. (2009). Kinetic controls on the
 826 complexation between mercury and dissolved organic matter in a contaminated environment.
 827 *Environ. Sci. Technol.*, 43(22), 8548-8553.
- 828 Mitchell, C. P. J., & Gilmour, C. C. (2008). Methylmercury production in a Chesapeake Bay salt marsh.
 829 *J. Geophys. Res.*, 113, G00C04, doi:10.1029/2008JG000765.
- 830 Mulholland, P. J., Best, G. R., Coutant, C. C., Hornberger, G. M., Meyer, J. L., Robinson, P. J., . . .
 831 Wetzel, R. G. (1997). Effects of climate change on freshwater ecosystems of the south-eastern
 832 United States and the Gulf Coast of Mexico. *Hydrological Processes*, 11(8), 949-970.
- 833 Naftz, D. L., Cederberg, J. R., Krabbenhoft, D. P., Beisner, K. R., Whitehead, J., & Gardberg, J. (2011).
 834 Diurnal trends in methylmercury concentration in a wetland adjacent to Great Salt Lake, Utah,
 835 USA. *Chem. Geol.*, 283(1-2), 78-86. doi:10.1016/j.chemgeo.2011.02.005
- 836 Ndu, U., Christensen, G. A., Rivera, N. A., Gionfriddo, C. M., Deshusses, M. A., Elias, D. A., & Hsu-
 837 Kim, H. (2018). Quantification of Mercury Bioavailability for Methylation Using Diffusive
 838 Gradient in Thin-Film Samplers. *Environmental Science & Technology*, 52(15), 8521-8529.
 839 doi:10.1021/acs.est.8b00647
- 840 Nimick, D. A., McCleskey, B. R., Gammons, C. H., Cleasby, T. E., & Parker, S. R. (2007). Diel mercury-
 841 concentration variations in streams affected by mining and geothermal discharge. *Sci. Tot.*
 842 *Environ.*, 373(1), 344-355. doi:10.1016/j.scitotenv.2006.11.008
- 843 Obrist, D., Kirk, J. L., Zhang, L., Sunderland, E. M., Jiskra, M., & Selin, N. E. (2018). A review of global
 844 environmental mercury processes in response to human and natural perturbations: Changes of
 845 emissions, climate, and land use. *Ambio*, 47(2), 116-140. doi:10.1007/s13280-017-1004-9
- 846 Olsen, T. A., Brandt, C. C., & Brooks, S. C. (2016). Periphyton Biofilms Influence Net Methylmercury
 847 Production in an Industrially Contaminated System. *Environ. Sci. Technol.*, 50(20), 10843-10850.
 848 doi:10.1021/acs.est.6b01538
- 849 Oswald, C. J., & Branfireun, B. A. (2014). Antecedent moisture conditions control mercury and dissolved
 850 organic carbon concentration dynamics in a boreal headwater catchment. *Water Resour. Res.*,
 851 50(8), 6610-6627. doi:10.1002/2013wr014736
- 852 Parr, P. D., & Hughes, J. F. (2006). *Oak Ridge Reservation: Physical Characteristics and Natural*
 853 *Resources. ORNL/TM-2006/110*. Retrieved from <http://www.osti.gov/bridge>
- 854 Qian, Y., Yin, X., Lin, H., Rao, B., Brooks, S. C., Liang, L., & Gu, B. (2014). Why Dissolved Organic
 855 Matter Enhances Photodegradation of Methylmercury. *Environmental Science & Technology*
 856 *Letters*, 1(10), 426-431. doi:10.1021/ez500254z
- 857 Riscassi, A., Miller, C., & Brooks, S. (2016). Seasonal and flow-driven dynamics of particulate and
 858 dissolved mercury and methylmercury in a stream impacted by an industrial mercury source.
 859 *Environ. Toxicol. Chem.*, 35(6), 1386-1400. doi:10.1002/etc.3310
- 860 Riscassi, A., Miller, C. L., & Brooks, S. C. (2014). Impact of collection container material and holding
 861 times on sample integrity for mercury and methylmercury in water. *Limnology and*
 862 *Oceanography-Methods*, 12, 407-420. doi:10.4319/lom.2014.12.407
- 863 Sankar, M. S., Dash, P., Lu, Y., Paul, V., Mercer, A. E., Arslan, Z., . . . Rodgers, J. C. (2019). Dissolved
 864 organic matter and trace element variability in a blackwater-fed bay following precipitation.
 865 *Estuarine, Coastal and Shelf Science*, 231, 106452.
 866 doi:<https://doi.org/10.1016/j.ecss.2019.106452>
- 867 Schuster, P. F., Shanley, J. B., Marvin-Dipasquale, M., Reddy, M. M., Aiken, G. R., Roth, D. A., . . .
 868 DeWild, J. F. (2008). Mercury and Organic Carbon Dynamics During Runoff Episodes from a
 869 Northeastern USA Watershed. *Water, Air, and Soil Pollution*, 187(1), 89-108.
 870 doi:10.1007/s11270-007-9500-3

- 871 Schwartz, G. E., Olsen, T. A., Muller, K. A., & Brooks, S. C. (2019). Ecosystem Controls on
 872 Methylmercury Production by Periphyton Biofilms in a Contaminated Stream: Implications for
 873 Predictive Modeling. *Environ. Toxicol. Chem.*, 38(11), 2426-2435. doi:10.1002/etc.4551
- 874 Scudder, B. C., Chasar, L. C., Wentz, D. A., Bauch, N. J., Brigham, M. E., Moran, P. W., & Krabbenhoft,
 875 D. P. (2009). *Mercury in Fish, Bed Sediment, and Water from Streams Across the United States, 1998-2005*. Retrieved from
 876
- 877 Selin, N. E. (2009). Global Biogeochemical Cycling of Mercury: A Review. *Annual Review of*
 878 *Environment and Resources*, 34, 43-63. doi:10.1146/annurev.enviro.051308.084314
- 879 Sellers, P., Kelly, C. A., Rudd, J. W. M., & MacHutchon, A. R. (1996). Photodegradation of
 880 methylmercury in lakes. *Nature*, 380(6576), 694-697. doi:10.1038/380694a0
- 881 Shiller, A. M., Duan, S., van Erp, P., & Bianchi, T. S. (2006). Photo-oxidation of dissolved organic matter
 882 in river water and its effect on trace element speciation. *Limnology and Oceanography*, 51(4),
 883 1716-1728. doi:10.4319/lo.2006.51.4.1716
- 884 Slowey, A. J. (2010). Rate of formation and dissolution of mercury sulfide nanoparticles: The dual role of
 885 natural organic matter. *Geochimica et Cosmochimica Acta*, 74(16), 4693-4708.
 886 doi:<https://doi.org/10.1016/j.gca.2010.05.012>
- 887 Southworth, G., Mathews, T., Greeley, M., Peterson, M., Brooks, S., & Kettle, D. (2013). Sources of
 888 mercury in a contaminated stream-implications for the timescale of recovery. *Environ. Toxicol.*
 889 *Chem.*, 32(4), 764-772. doi:10.1002/etc.2115
- 890 Tsui, M. T. K., Finlay, J. C., Balogh, S. J., & Nollet, Y. H. (2010). In Situ Production of Methylmercury
 891 within a Stream Channel in Northern California. *Environ. Sci. Technol.*, 44(18), 6998-7004.
 892 doi:10.1021/es101374y
- 893 U. S. EPA. (2001). *Method 1630: Methyl Mercury in Water by Distillation, Aqueous Ethylation, Purge*
 894 *and Trap, and CVAFS*. Retrieved from [https://www.epa.gov/sites/production/files/2015-](https://www.epa.gov/sites/production/files/2015-08/documents/method_1630_1998.pdf)
 895 [08/documents/method_1630_1998.pdf](https://www.epa.gov/sites/production/files/2015-08/documents/method_1630_1998.pdf)
- 896 U. S. EPA. (2002). *Method 1631, Revision E: Mercury in Water by Oxidation, Purge and Trap, and Cold*
 897 *Vapor Atomic Fluorescence Spectrometry*. Retrieved from
 898 https://www.epa.gov/sites/production/files/2015-08/documents/method_1631e_2002.pdf
- 899 United Nations Environment Programme Global Mercury Partnership. (2020). *Overarching Framework*
 900 *for the UNEP Global Mercury Partnership*. Retrieved from
 901 [https://web.unep.org/globalmercurypartnership/overarching-framework-unep-global-mercury-](https://web.unep.org/globalmercurypartnership/overarching-framework-unep-global-mercury-partnership-version-june-2020)
 902 [partnership-version-june-2020](https://web.unep.org/globalmercurypartnership/overarching-framework-unep-global-mercury-partnership-version-june-2020)
- 903 Waples, J. S., Nagy, K. L., Aiken, G. R., & Ryan, J. N. (2005). Dissolution of cinnabar (HgS) in the
 904 presence of natural organic matter. *Geochim. Cosmochim. Acta*, 69(6), 1575-1588.
- 905 Wei, Q. S., Feng, C. H., Wang, D. S., Shi, A. Y., Zhang, L. T., Wei, Q., & Tang, H. X. (2008). Seasonal
 906 variations of chemical and physical characteristics of dissolved organic matter and trihalomethane
 907 precursors in a reservoir: a case study. *Journal of Hazardous Materials*, 150(2), 257-264.
 908 doi:10.1016/j.jhazmat.2007.04.096
- 909 Weishaar, J. L., Aiken, G. R., Bergamaschi, B. A., Fram, M. S., Fujii, R., & Mopper, K. (2003).
 910 Evaluation of specific ultraviolet absorbance as an indicator of the chemical composition and
 911 reactivity of dissolved organic carbon. *Environ. Sci. Technol.*, 37(20), 4702-4708.
- 912 Wentz, D. A., Brigham, M. E., Chasar, L. C., Lutz, M. A., & Krabbenhoft, D. P. (2014). *Mercury in the*
 913 *Nation's streams – Levels, trends, and implications*. U.S. Geological Survey Circular 1395.
 914 Retrieved from <http://dx.doi.org/10.3133/cir1395>
- 915 Whyte, D. C., & Kirchner, J. W. (2000). Assessing water quality impacts and cleanup effectiveness in
 916 streams dominated by episodic mercury discharges. *Science of The Total Environment*, 260(1), 1-
 917 9. doi:[https://doi.org/10.1016/S0048-9697\(00\)00537-4](https://doi.org/10.1016/S0048-9697(00)00537-4)
- 918 Zhang, T., Kim, B., Levard, C., Reinsch, B. C., Lowry, G. V., Deshusses, M. A., & Hsu-Kim, H. (2011).
 919 Methylation of Mercury by Bacteria Exposed to Dissolved, Nanoparticulate, and Microparticulate
 920 Mercuric Sulfides. *Environmental Science & Technology*, 46(13), 6950-6958.
 921 doi:10.1021/es203181m

922

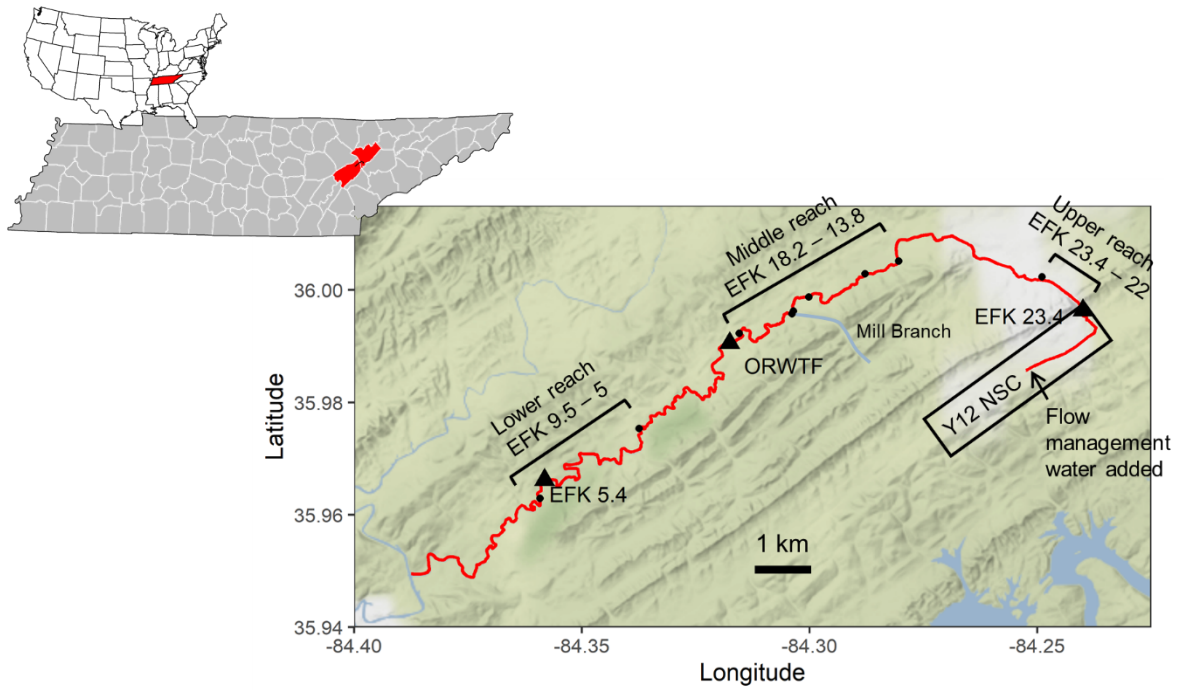


Figure 1. Map of East Fork Poplar Creek, shown in red with sampling locations marked by symbols. Discharge histories are given in Supporting Information for the three points marked with a triangle. The three marked creek reaches (upper, middle, and lower) indicate reaches for which data were aggregated in the presentation of results.

923

924

925

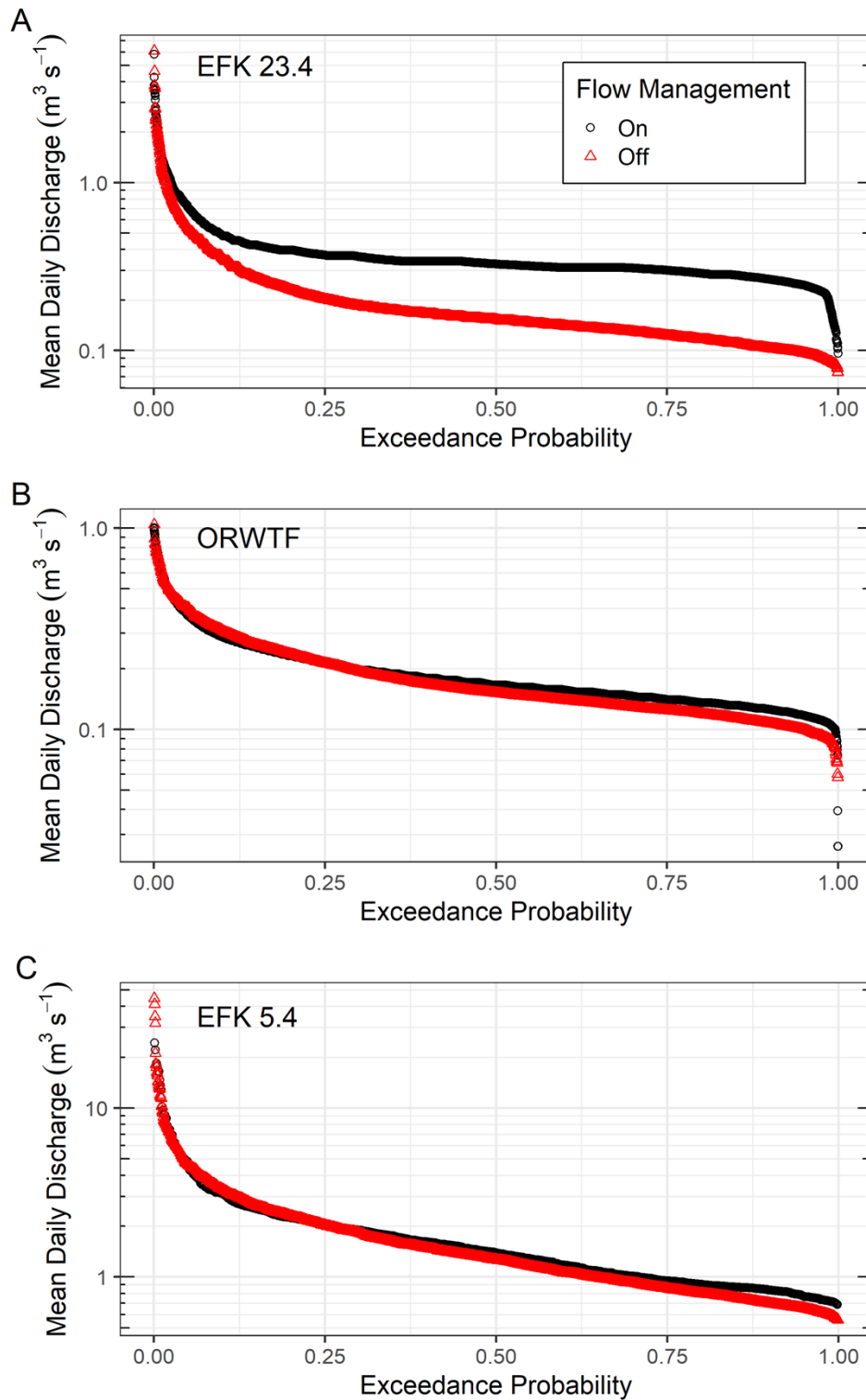


Figure 2. Mean daily discharge flow exceedance probabilities during and after active flow management at EFK 23.4 (A), the ORWTF outfall (B), and EFK 5.4 (C).

928

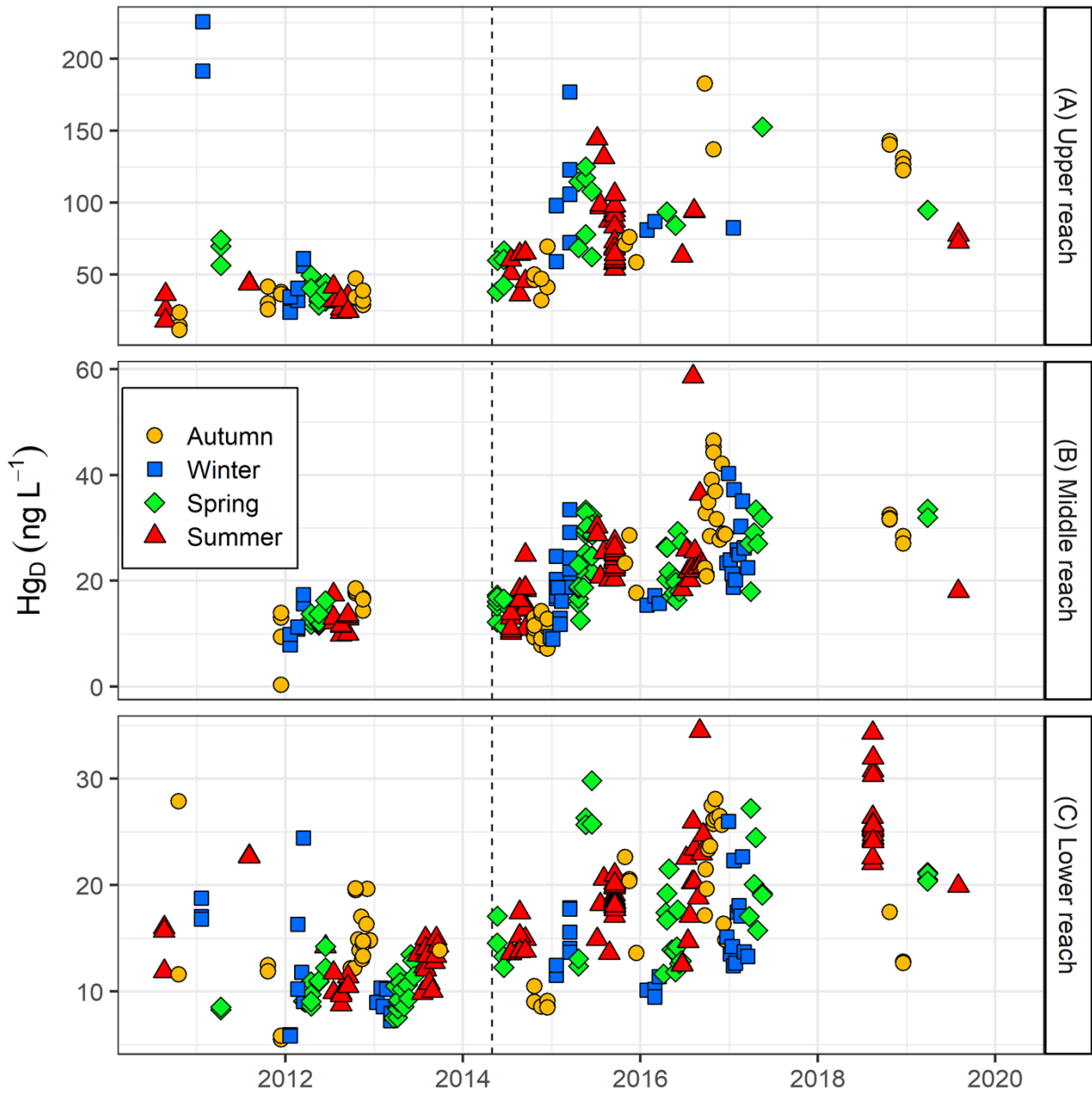


Figure 3. Total dissolved Hg concentration over time in each of the three creek reaches. Vertical dashed line indicates the end of flow management.

929
930
931

932

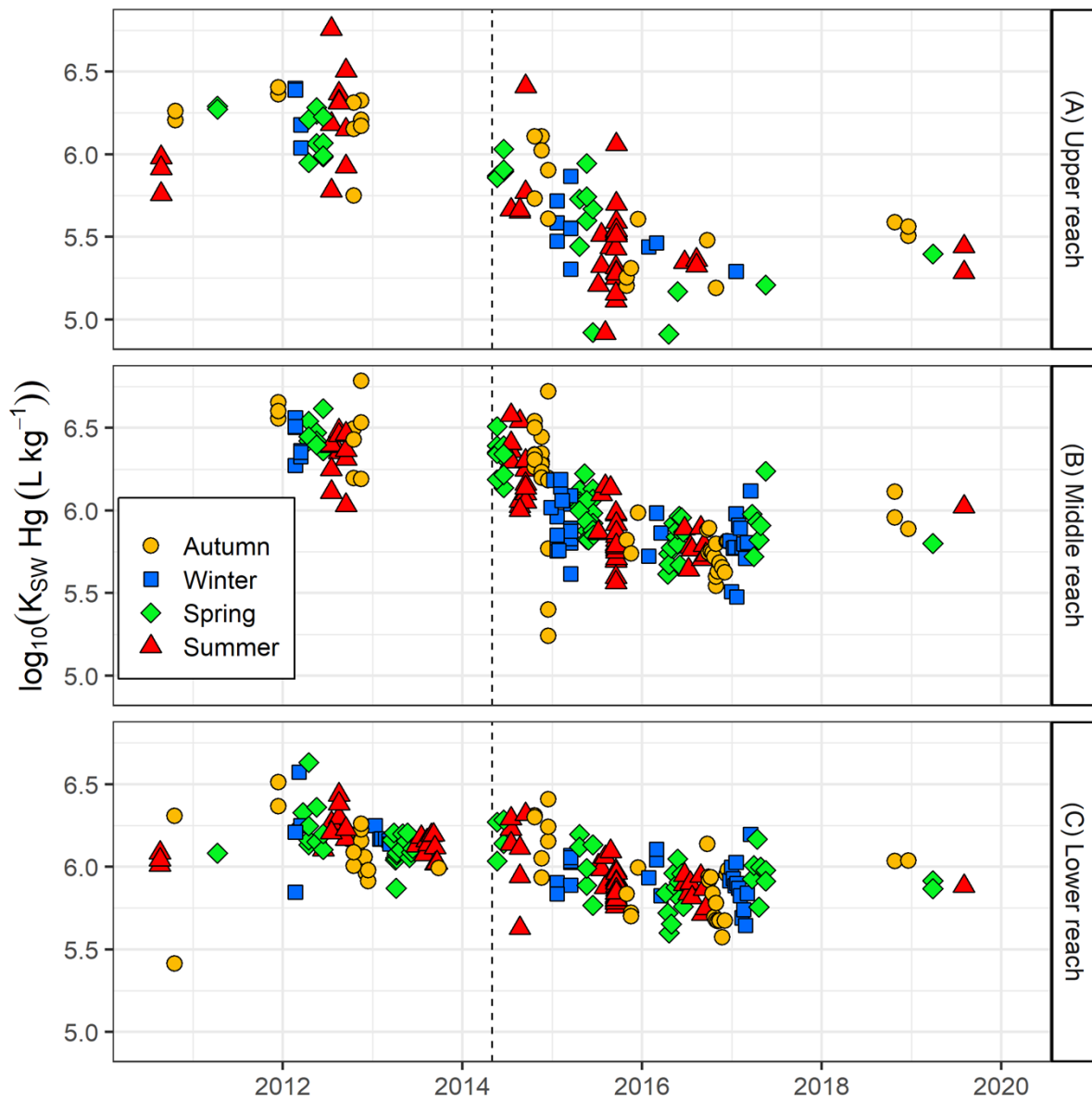


Figure 4. Hg solid-water partitioning coefficient in each creek reach over time. Vertical dashed line indicates the end of flow management.

933
934
935

936

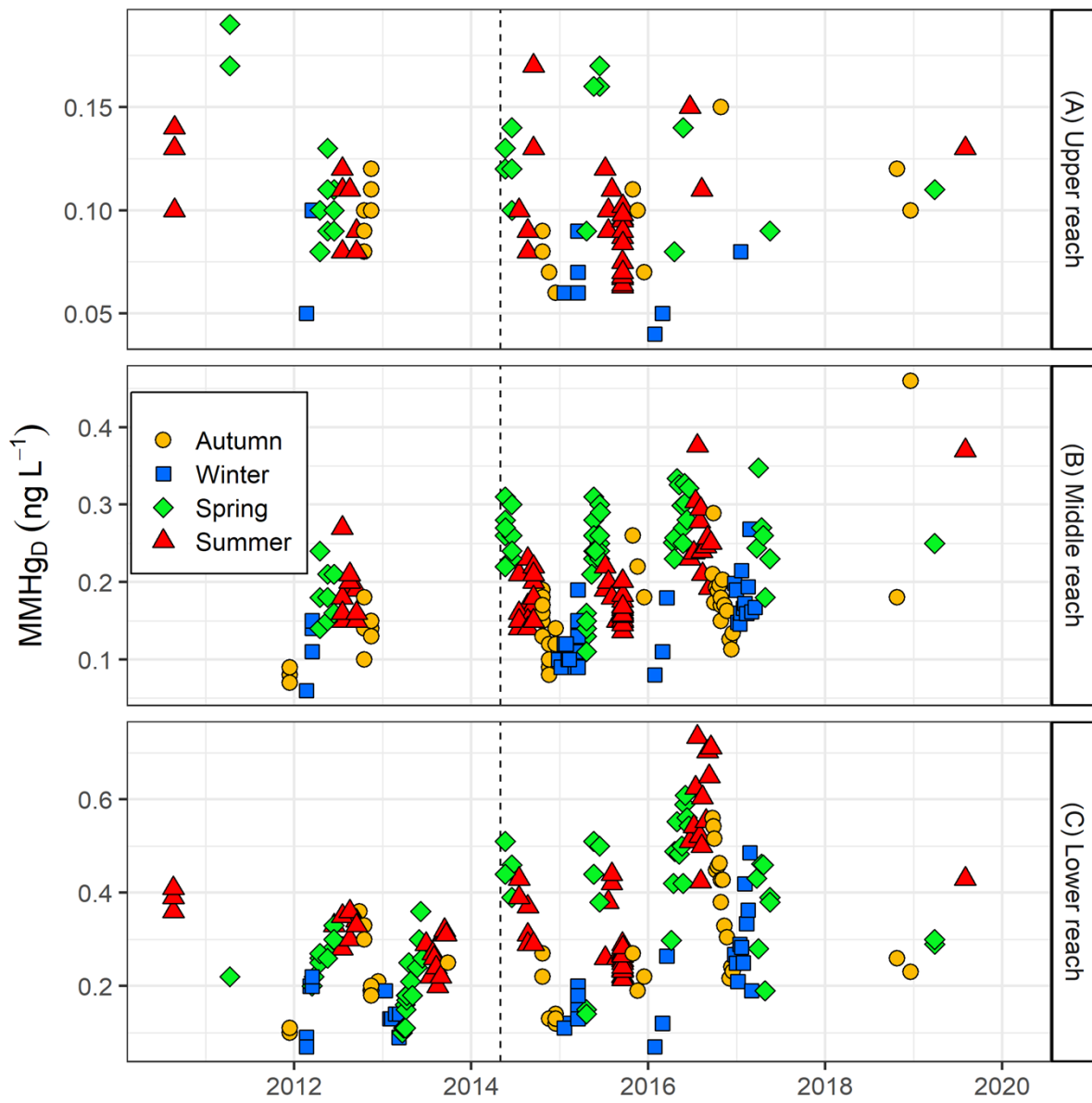


Figure 5. Dissolved MMHg concentration over time in each of the three creek reaches. Vertical dashed line indicates the end of flow management.

937
938
939

940

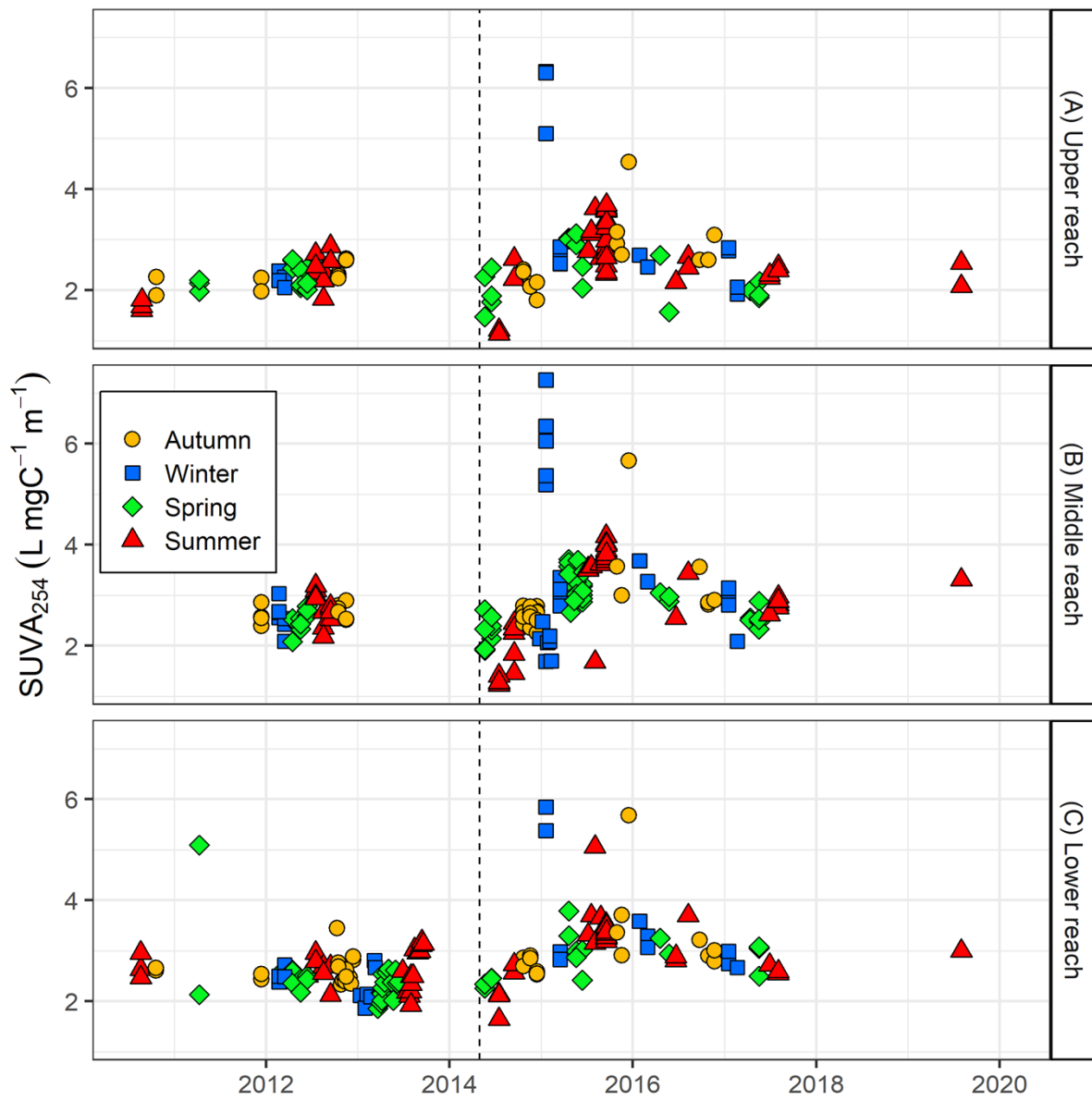


Figure 6. SUVA₂₅₄ values for each creek reach over time. Vertical dashed line indicates the end of flow management.

941

942

943

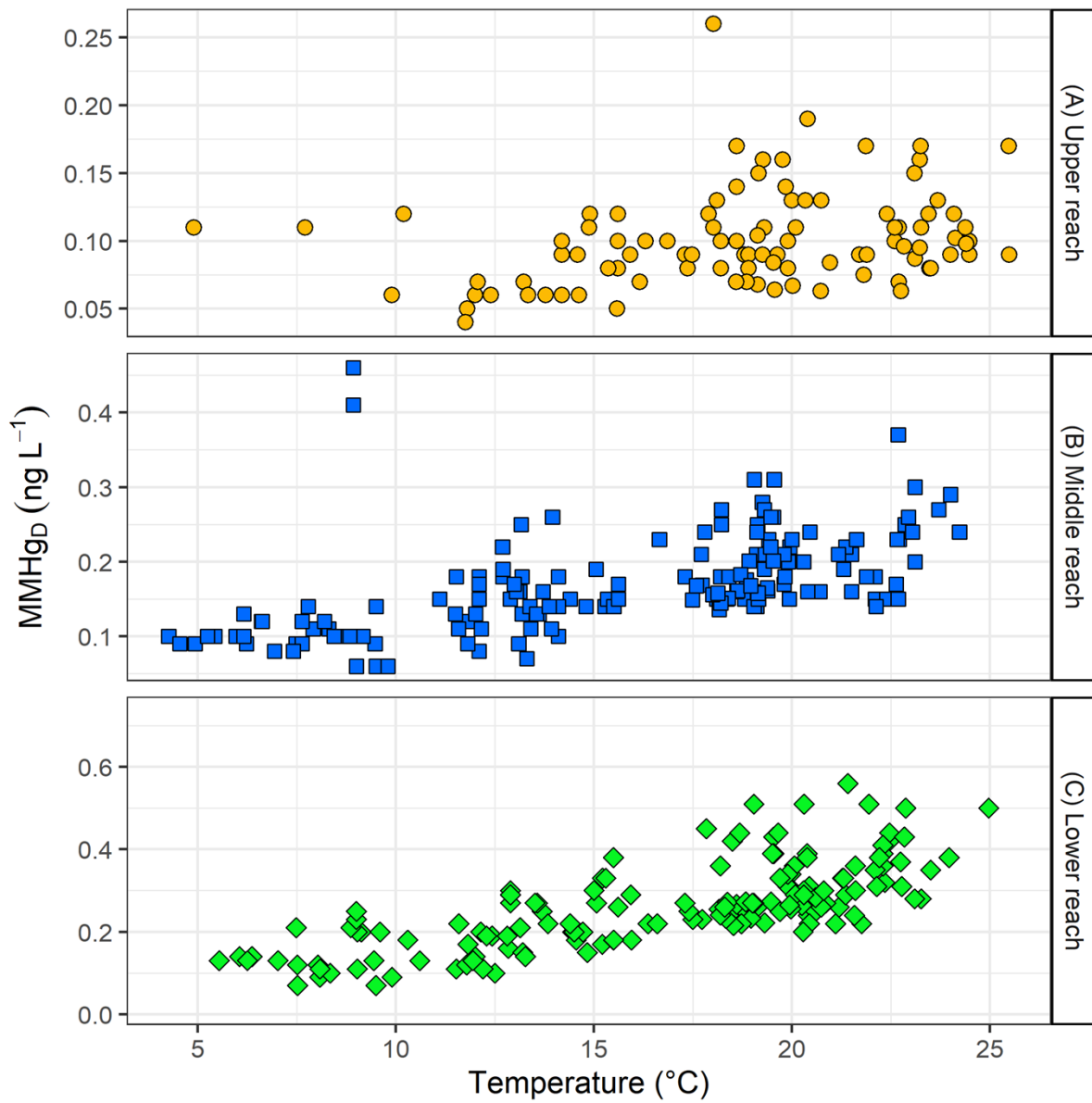


Figure 7. Dissolved MMHg concentration versus water temperature at the time of sampling in each creek reach. MMHg_D concentration is low, relatively constant at ~0.12 ng L⁻¹, and independent of temperature for all reaches at temperatures below 10°C and significantly positively correlated with temperature above that threshold (see Table S7).

944

945